the possibilities that some other mechanisms are also involved in the growth-inhibitory effects of ANP in cardiomyocytes.

Although a variety of molecules that promote the development of cardiac hypertrophy have been well examined [3–8], little is known about the molecules that inhibit cardiac hypertrophy. ANP is quite unique in that it exhibits growth-inhibitory effects on cardiomyocytes. Simultaneous induction of both growth-promoting and growth-inhibiting factors in the myocardium suggests that cardiac growth in response to hemodynamic overload is controlled by complex regulatory mechanisms. Although the precise mechanism by which ANP inhibits the development of cardiac hypertrophy remains to be further clarified, understanding the physiological and pathological actions of ANP on cardiac cells may allow the development of novel therapeutic strategies for modulating the hypertrophy of cardiomyocytes and the overall remodeling of the myocardium.

References

[1] A.M. Katz, Cardiomyopathy of overload. A major determinant of prognosis in congestive heart failure, N. Engl. J. Med. 322 (1990) 100–110.
[2] D. Levy, R.J. Garrison, D.D. Savage, W.B. Kannel, W.P. Castelli, Prognostic implications of echocardiographically determined left ventricular mass in the Framingham heart study, N. Engl. J. Med. 332 (1990) 1561–1566.
[3] I. Komuro, Y. Yazaki, Control of cardiac gene expression by mechanical stress, Annu. Rev. Physiol. 55 (1993) 55–75.
[4] K.M. Baker, J.F. Aceto, Angiotensin II stimulation of protein synthesis and cell growth in chick heart cells, Am. J. Physiol. 259 (1990) H610–H618.
[5] J. Sadoshima, Z. Qiu, J.P. Morgan, S. Izumo, Angiotensin II and other hypertrophic stimuli mediated by G protein-coupled receptors activate tyrosine kinase, mitogen-activated protein kinase, and 90-kD S6 kinase in cardiac myocytes: the critical role of Ca^{2+}-dependent signaling, Circ. Res. 76 (1995) 1–15.
[6] M. Kojima, I. Shiojima, T. Yamazaki, I. Komuro, Y. Zou, W. Ying, T. Mizuno, K. Ueki, K. Tobe, T. Kadowaki, R. Nagai, Y. Yazaki, Angiotensin II receptor antagonist TCV-116 induces regression of hypertensive left ventricular hypertrophy in vivo and inhibits the intracellular signaling pathway of stretch-mediated cardiomyocyte hypertrophy in vivo, Circulation 89 (1994) 2204–2211.
[7] T. Yamazaki, I. Komuro, S. Kudoh, Y. Zou, I. Shiojima, T. Mizuno, H. Takano, Y. Hiroi, K. Ueki, K. Tobe, T. Kadowaki, Y. Yazaki, Angiotensin II partly mediates mechanical stress-induced cardiac hypertrophy, Circ. Res. 77 (1995) 258–265.
[8] H. Ito, M. Hiroe, Y. Hirata, H. Fujisaki, S. Adachi, H. Akimoto, Y. Ohta, F. Marumo, Endothelin ETA receptor antagonist blocks cardiac hypertrophy provoked by hemodynamic overload, Circulation 89 (1994) 2198–2203.
[9] T. Yamazaki, I. Komuro, S. Kudoh, Y. Zou, I. Shiojima, Y. Hiroi, T. Mizuno, K. Maemura, H. Kurihara, R. Aikawa, H. Takano, Y. Yazaki, Endothelin-1 is involved in mechanical stress-induced cardiomyocyte hypertrophy, J. Biol. Chem. 271 (1996) 3221–3228.
[10] J. Thorburn, J.A. Frost, A. Thorburn, Mitogen-activated protein kinases mediate changes in gene expression, but not cytoskeletal organization associated with cardiac muscle cell hypertrophy, J. Cell Biol. 126 (1994) 1565–1572.
[11] J. Thorburn, M. Carlson, S.J. Mansour, K.R. Chien, N.G. Ahn, A. Thorburn, Inhibition of a signaling pathway in cardiac muscle cells by active mitogen-activated protein kinase kinase, Mol. Biol. Cell. 6 (1995) 1479–1490.
[12] P.E. Glennon, S. Kadoura, E.M. Sale, G.J. Sale, S.J. Fuller, P.H. Sugden, Depletion of mitogen-activated protein kinase using an antisense oligodeoxynucleotide approach downregulates the phenylephrine-induced hypertrophic response in rat cardiac myocytes, Circ. Res. 78 (1996) 954–961.
[13] H. Ruskoaho, Atrial natriuretic peptide: synthesis, release, and metabolism, Pharmcol. Rev. 44 (1992) 479–602.
[14] U.C. Garg, A. Hassid, Nitric oxide-generating vasodilators and 8-bromo-cyclic guanosine monophosphate inhibit mitogenesis and proliferation of cultured rat vascular smooth muscle cells, J. Clin. Invest. 83 (1989) 1774–1777.
[15] M. Kohno, M. Ikeda, M. Johchi, T. Horio, K. Yasunari, N. Kurihara, T. Takeda, Interaction of PDGF and natriuretic peptides on mesangial cell proliferation and endothelin secretion, Am. J. Physiol. 265 (1993) E673–E679.
[16] R. Morishita, G.H. Gibbons, R.E. Pratt, N. Tomita, Y. Kaneda, T. Ogihara, V.J. Dzau, Autocrine and paracrine effects of atrial natriuretic peptide gene transfer on vascular smooth muscle and endothelial cellular growth, J. Clin. Invest. 94 (1995) 824–829.
[17] L. Cao, D.G. Gardner, Natriuretic peptides inhibit DNA synthesis in cardiac fibroblasts, Hypertension 25 (1995) 227–234.
[18] S.M. Yu, L.M. Hung, C.C. Lin, cGMP-elevating agents suppress proliferation of vascular smooth muscle cells by inhibiting the activation of epidermal growth factor signaling pathway, Circulation 95 (1997) 1269–1277.
[19] B.A. Prins, M.J. Weber, R.M. Hu, A. Pedram, M. Daniels, E.R. Levin, Atrial natriuretic peptide inhibits mitogen-activated protein kinase through the clearance receptor. Potential role in the inhibition of astrocyte proliferation, J. Biol. Chem. 271 (1996) 14156–14162.
[20] T. Sugimoto, M. Haneda, M. Togawa, M. Isono, T. Shikano, S. Araki, T. Nakagawa, A. Kashiwagi, K.L. Guan, R. Kikkawa, Atrial natriuretic peptide induces the expression of MKP-1, a mitogen-activated protein kinase phosphatase, in glomerular mesangial cells, J. Biol. Chem. 271 (1996) 544–547.
[21] H. Sun, C.H. Charles, L.F. Lau, N.K. Tonks, MKP-1 (3CH134), an immediate early gene product, is a dual specificity phosphatase that dephosphorylates MAP kinase in vivo, Cell 75 (1993) 487–493.
[22] S.J. Fuller, E.L. Davies, J. Gillespie-Brown, H. Sun, N.K. Tonks, Mitogen-activated protein kinase phosphatase 1 inhibits the stimulation of gene expression by hypertrophic agonists in cardiac myocytes, Biochem. J. 323 (1997) 313–319.
[23] H. Sun, N.K. Tonks, D. Bar-Sagi, Inhibition of Ras-induced DNA synthesis by expression of the phosphatase MKP-1, Science 266 (1994) 285–288.
[24] Y. Liu, M. Gorospe, C. Yang, N.J. Holbrook, Role of mitogen-activated protein kinase phosphatase during the cellular response to genotoxic stress. Inhibition of c-Jun N-terminal kinase activity and AP-1-dependent gene activation, J. Biol. Chem. 270 (1995) 8377–8380.
[25] I. Komuro, S. Kudoh, T. Yamazaki, Y. Zou, I. Shiojima, Y. Yazaki, Mechanical stretch activates the stress-activated protein kinases in cardiac myocytes, FASEB J. 10 (1996) 631–636.
[26] S. Kudoh, I. Komuro, Y. Hiroi, Y. Zou, K. Harada, T. Sugaya, N. Takekoshi, K. Murakami, T. Kadowaki, Y. Yazaki, Mechanical stretch induces hypertrophic responses in cardiac myocytes of angiotensin II type 1a receptor knockout mice, J. Biol. Chem. 273 (1998) 24037–24043.

[27] S. Nemoto, Z. Sheng, A. Lin, Opposing effects of Jun kinase and p38 mitogen-activated protein kinases on cardiomyocyte hypertrophy, Mol. Cell. Biol. 18 (1998) 3518–3526.
[28] D. Zechner, D.J. Thuerauf, D.S. Hanford, P.M. McDonough, C.C. Glembotski, A role for the p38 mitogen-activated protein kinase pathway in myocardial cell growth, sarcomeric organization, and cardiac-specific gene expression, J. Cell Biol. 139 (1997) 115–127.
[29] A. Clerk, A. Michael, P.H. Sugden, Stimulation of the p38 mitogen-activated protein kinase pathway in neonatal rat ventricular myocytes by the G protein-coupled receptor agonists, endothelin-1 and phenylephrine: a role in cardiac myocyte hypertrophy?, J. Cell Biol. 142 (1998) 523–535.
[30] Y. Wang, B. Su, V.P. Sah, J.H. Brown, J. Han, K.R. Chien, Cardiac hypertrophy induced by mitogen-activated protein kinase kinase 7, a specific activator for c-Jun NH2-terminal kinase in ventricular muscle cells, J. Biol. Chem. 273 (1998) 5423–5426.
[31] K. Harada, I. Komuro, I. Shiojima, D. Hayashi, S. Kudoh, T. Mizuno, K. Kijima, H. Matsubara, T. Sugaya, K. Murakami, Y. Yazaki, Pressure overload induces cardiac hypertrophy in angiotensin II type 1A receptor knockout mice, Circulation 97 (1998) 1952–1959.
[32] D.R. Alessi, C. Smythe, S.M. Keyse, The human CL100 gene encodes a Tyr/Thr-protein phosphatase which potently and specifically inactivates MAP kinase and suppresses its activation by oncogenic ras in *Xenopus* oocyte extracts, Oncogene 8 (1993) 2015–2020.
[33] M. Isono, M. Haneda, S. Maeda, M. Omatsu-Kanbe, R. Kikkawa, Atrial natriuretic peptide inhibits endothelin-1-induced activation of JNK in glomerular mesangial cells, Kidney Int. 53 (1998) 1133–1142.
[34] A.C. Rosenkranz, R.L. Woods, G.J. Dusting, R.H. Ritchie, Antihypertrophic actions of the natriuretic peptides in adult rat cardiomyocytes: importance of cyclic GMP, Cardiovasc. Res. 57 (2003) 515–522.
[35] C. Angelino, M.T. Cynthia, T. Nobuyuki, L.F.C. Donny, S.C. Wilson, Nitric oxide, atrial natriuretic peptide, and cyclic GMP inhibit the growth-promoting effects of norepinephrine in cardiac myocytes and fibroblasts, J. Clin. Invest. 101 (1998) 812–818.

Double Aortic Arch With a Compressed Trachea Demonstrated by Multislice Computed Tomography

Nobusada Funabashi, MD; Atsushi Ishida, MD; Katsuya Yoshida, MD; Issei Komuro, MD

A 33-year-old man had a chest x-ray that showed an abnormal enlargement of the thoracic aorta. ECG-gated enhanced multislice computed tomography (CT) (Light Speed Ultra 16, General Electric) was therefore performed with a 0.625-mm slice thickness and a helical pitch of 3.25. Thirty seconds after intravenous injection of 100 mL of iodinated contrast material (350 mgI/mL), CT scanning was performed with retrospective ECG-gated reconstruction and volume data were transferred to a workstation (Virtual Place Office, Azemoto, Tokyo, Japan).

Axial source images (Figure 1A) and multiplanar reconstruction images of the coronal view (Figure 1B) revealed separated right and left aortic arches and a trachea and esophagus surrounded by a vascular ring made by the double aortic arches. The trachea was actually slightly compressed by the vascular ring (Figure 1B, arrowhead). Three-dimensional volume rendering images also revealed the double aortic arch, which was separated at the distal portion of the ascending aorta (Figure 2A) and joined at the proximal portion of the descending aorta (Figure 2B). The right subclavian artery and right common carotid artery both originated separately from the right aortic arch, and the left subclavian artery and left common carotid artery originated from the left aortic arch. Because the patient did not experience symptoms of compression of the esophagus or trachea, surgical intervention is not currently planned.

Acknowledgments

This work was supported by Japan Cardiovascular Research Foundation.

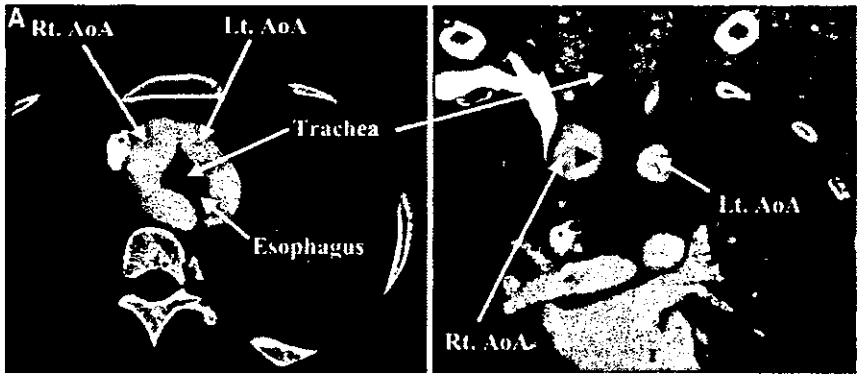

Figure 1. Axial source image (A) and multiplanar reconstruction image from the coronal view (B) of enhanced multislice CT revealed separate right (rt.) and left (lt.) aortic arches (AoA). The trachea and esophagus were surrounded by a vascular ring made by the double AoA (A), and the trachea was actually slightly compressed by the vascular ring (B, arrowheads).

From the Departments of Cardiovascular Science and Medicine (N.F., K.Y., I.K.) and General Surgery (A.I.), Chiba University Graduate School of Medicine, Chiba, Japan.

Correspondence to Issei Komuro, MD, Department of Cardiovascular Science and Medicine, Chiba University Graduate School of Medicine, 1-8-1 Inohana, Chuo-ku, Chiba City, Chiba 260-8670, Japan. E-mail komuro-tky@umin.ac.jp

(*Circulation.* 2004;110:e68-e69.)

Circulation is available at http://www.circulationaha.org

DOI: 10.1161/01.CIR.0000138742.98726.5F

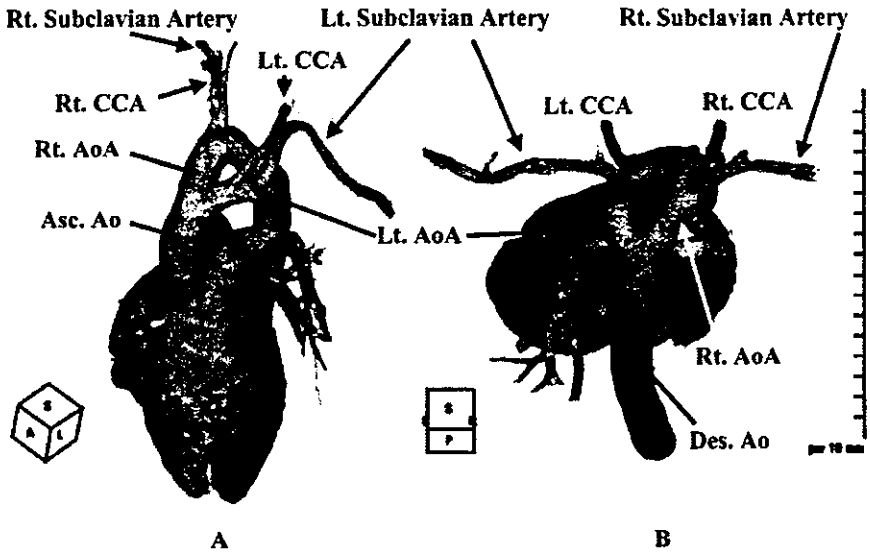

Figure 2. Three-dimensional volume rendering image of enhanced multislice CT from the left superior anterior view (A) and from the superior posterior view (B) revealed double aortic arches (AoA) separated at the distal portion of the ascending aorta (Asc. Ao) (A) and joined at the proximal portion of the descending aorta (Des. Ao) (B). The right (rt.) subclavian artery and right common carotid artery (CCA) originated separately from the right aortic arch (rt. AoA), and the left (lt.) subclavian artery and left CCA originated from the left aortic arch (lt. AoA). PA indicates pulmonary artery; RV, right ventricle; and LV, left ventricle.

J Pharmacol Sci 96, 23 – 26 (2004)

Journal of Pharmacological Sciences

Forum Minireview

Forefront of Na^+/Ca^{2+} Exchanger Studies: Role of Na^+/Ca^{2+} Exchanger – Lessons From Knockout Mice

Issei Komuro[1,*] and Masashi Ohtsuka[1]

[1]*Department of Cardiovascular Science and Medicine, Chiba University Graduate School of Medicine, 1-8-1 Inohana, Chuo-ku, Chiba 260-8670, Japan*

Received June 14, 2004; Accepted July 27, 2004

Abstract. We used Na^+/Ca^{2+} exchanger (NCX) knockout mice to evaluate the effects of NCX in cardiac function and the infarct size after ischemia/reperfusion injury. The contractile function in NCX KO mice hearts was significantly better than that in wild type (WT) mouse hearts after ischemia/reperfusion and the infracted size was significantly smaller in NCX KO mice hearts compared with that in WT mice hearts. NCX is critically involved in the development of ischemia/reperfusion-induced myocardial injury, and therefore the inhibition of NCX function may contribute to cardioprotection against ischemia/reperfusion injury.

Keywords: Na^+/Ca^{2+} exchanger (NCX), knockout mouse, heart, ischemia/reperfusion injury

Introduction

The Na^+/Ca^{2+} exchanger (NCX) is an important electrogenic transporter in maintaining calcium homeostasis in a variety of mammalian organs (1). NCX catalyzes electrogenic exchange of Na^+ and Ca^{2+} across the plasma membrane in either the Ca^{2+}-efflux (the forward mode) or Ca^{2+}-influx (the reverse mode), depending on the electrochemical gradients of the substrate ions. In the heart, NCX plays an important role in excitation-contraction coupling as the dominant myocardial Ca^{2+}-efflux system (2). On the other hand, the reverse mode of NCX is associated with in cytoplasmic Ca^{2+} levels in cardiomyocytes during digitalis treatment or ischemia/reperfusion (3). It has been reported that NCX inhibitors and NCX antisense oligonucleotides protect the heart from ischemia/reperfusion injury (4, 5). However, two putative NCX inhibitors, KB-R7943 and SEA0400, have been reported to be not specific for NCX (6). Therefore, it remains unclear whether NCX indeed plays a crucial role in mediating Ca^{2+} influx that leads to Ca^{2+} overload and cellular injury after myocardial ischemia, reperfusion injury.

We generated *Ncx1*-deficient mice by gene targeting to determine the in vivo function of the exchanger (7). Homozygous *Ncx1*-deficient mice died between embryonic days 9 and 10. Their hearts did not beat, and cardiac myocytes showed apoptosis. No forward mode or reverse mode of the Na^+/Ca^{2+} exchange activity was detected in null mutant hearts. The Na^+-dependent Ca^{2+} exchange activity as well as protein content of NCX1 were decreased by approximately 50% in the heart, kidney, aorta, and smooth muscle cells of the heterozygous mice, and tension development of the aortic ring in Na^+-free solution was markedly impaired in heterozygous mice. These findings suggest that NCX1 is required for heartbeats and survival of cardiac myocytes in embryos and plays critical roles in Na^+-dependent Ca^{2+} handling in the heart and aorta.

*Corresponding author. FAX: +81-43-226-2557
E-mail: komuro-tky@umin.ac.jp

The functional activity as well as the protein content of NCX in the myocardium of NCX KO mice is approximately half of those of WT mice

Twelve-week-old male heterozygous knockout (KO) mice and wild type (WT) littermates were used. All animal experiments were performed according to the Guide for the Care and Use of Laboratory Animals (NIH publication No. 85-23, revised 1996). Ventricular cells were prepared from adult mouse hearts by standard enzymatic digestion (8). Whole-cell membrane currents were recorded by the patch-clamp method and the current-voltage relationship was obtained by voltage clamp ramp pulses as described previously (9). Under

these conditions, the Ni^{2+}-sensitive current represents NCX current (10). All data were acquired and analyzed by the pCLAMP (version 5.5; Axon Instrument) software.

Expression levels of dihydropyridine (DHP) receptor (L-type Ca^{2+} channel) and SR Ca^{2+}-ATPase 2 (SERCA2) were analyzed by Western blot as described previously (11). Briefly, tissue was homogenized in lysis buffer containing 25 mM Tris-HCl (pH 7.4), 25 mM NaCl, 0.5 mM EGTA, 10 mM sodium pyrophosphate, 1 mM sodium orthovanadate, 10 mM NaF, 10 nM okadaic acid, 1 mM PMSF, 20 μg/ml aprotinin, and 20 μg/ml leupeptin. Protein concentration was determined using a protein assay kit (BioRad, Hercules, CA, USA) and equal amounts of total protein (40 μg/lane) were separated on 8% SDS-polyacrylamide gel. Separated proteins were transferred to nitrocellulose membrane (Amersham Life Science, Arlington Heights, IL, USA). Membranes were incubated with anti-mouse dihydropyridine L-type Ca^{2+} channel α-2 subunit monoclonal antibody (Affinity Bioreagents, Inc., Golden, CO, USA) or anti-mouse SERCA2 monoclonal antibody (Affinity Bioreagents) at 4°C overnight. After washing, the membranes were incubated with horseradish peroxidase-conjugated goat anti-mouse antibody for 1 h. Immunoreactive protein was visualized using an enhanced chemiluminescence detection kit (ECL, Amersham).

We previously reported that the protein content of NCX in NCX KO mouse hearts was approximately 50% of that in WT mouse hearts (12). To elucidate the functional activity, we examined NCX current densites from −40 mV to 40 mV in WT (n = 9) and NCX KO ventricular cells (n = 6) (Fig. 1). The densities of the reverse mode of NCX at 40 mV in ventricular cells of KO mice (0.57 ± 0.07 pA/pF) were approximately half (55.4%) compared with those of WT mice (1.04 ± 0.14 pA/pF). These results suggest that the functional activity as well as the protein content of NCX in the myocardium of NCX KO mice is approximately half of those of WT mice.

Western blot analysis revealed that there was no difference in the protein levels of L-type Ca^{2+} channel and SERCA2 between the two groups (data not shown).

The infarct size was significantly smaller in KO hearts than in WT hearts

Hearts were excised from mice and connected to the perfusion canula via the aorta as described previously (8). Retrograde perfusion was maintained with Krebs-Henseleit solution. To evaluate the contractile function, a polyethylene film balloon was inserted into the cavity of the left ventricle through the left atrium. The balloon was filled with saline to adjust the baseline end-diastolic pressure to 5 – 10 mmHg. Hearts were subjected to no-flow, global ischemia by clamping the perfusion line. After 30 min of ischemia, the clamp was released and the hearts were reperfused for 120 min. Left ventricular developed pressure (LVDP) was designated as difference between systolic and diastolic pressures of the left ventricle. After 120 min, the heart was incubated for 5 min at 37°C in a 1% solution of triphenyltetrazolium chloride (TTC). The sizes of the infarcted area and viable ischemic-reperfused area were measured by computed planimetry (Scion Image 1.62; Scion Corporation, Frederick, MD, USA). Infarct size was calculated as described previously (13).

There were no significant differences in the basal hemodynamic parameters, including heart rate, left ventricular pressure, end-diastolic pressure, and positive and negative dP/dt, between WT and KO mice (Table 1). After ischemia, there was no significant difference between the two groups in several parameters such as time to no beating, time to contracture, and left

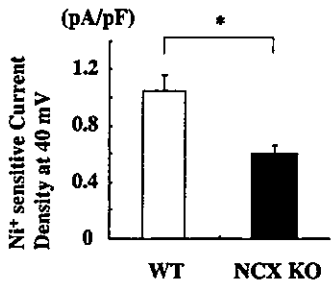

Fig. 1. NCX current densities. The densities of the reverse mode of NCX at 40 mV in ventricular myocytes isolated from WT (n = 9) and NCX KO mice hearts (n = 6). Values are expressed as the mean ± S.E.M. *P<0.05 *vs* WT mice.

Table 1. Hemodynamic parameters of NCX KO mice

	WT (n = 6)	NCX KO (n = 7)
HR (bpm)	356 ± 40	378 ± 77
LVP (mmHg)	142.8 ± 40	146.3 ± 34.5
EDP (mmHg)	4.4 ± 1.5	4.3 ± 1.3
dP/dt (mmHg/s)	7368 ± 630	7845 ± 2582
−dP/dt (mmHg/s)	5204 ± 782	5539 ± 1157
Time to no beating (min)	2.2 ± 0.9	2.2 ± 1.6
Time to contracture (min)	6.2 ± 1.7	6.3 ± 2.0
EDP at 25 min (mmHg)	67.3 ± 9.2	63.8 ± 10.8

HR, heart rate; LVP, left ventricular pressure; EDP, LV end-diastolic pressure; dP/dt and −dP/dt, positive and negative first derivatives for maximal rates of LV pressure development, respectively.

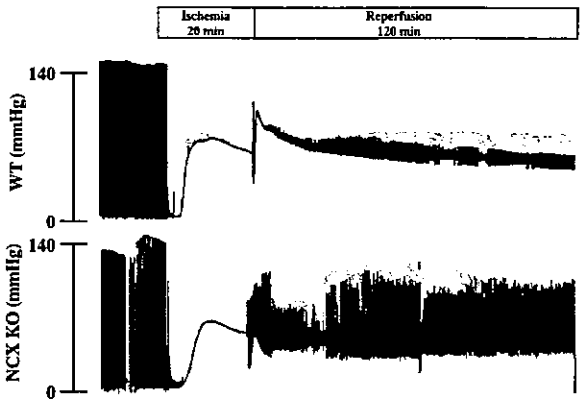

Fig. 2. Ex vivo studies. Changes in LVP during ischemia/reperfusion. Representative LVP records of WT and NCX KO mouse hearts are shown. Note that KO mouse hearts started to contract earlier than WT mouse hearts after reperfusion.

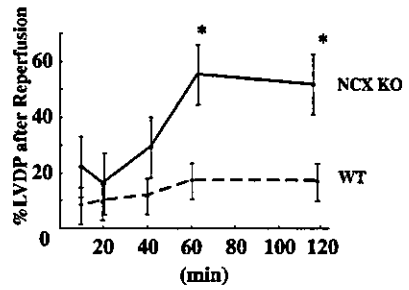

Fig. 3. LVDP of hearts of NCX KO mice (n = 7) and WT mice (n = 6) hearts after reperfusion. Values are expressed as the mean ± S.E.M. **P*<0.05 *vs* WT mice.

ventricular end-diastolic pressure (Fig. 2). After reperfusion, however, hearts of KO mice started to beat earlier than those of WT mice (Fig. 2). At 120 min after reperfusion, contractile function (left ventricular developed pressure) of KO mouse hearts was significantly better (51.7 ± 12.7% of preischemic value) than that of WT mouse hearts (26.3 ± 6.9%, $P<0.05$) (Fig. 3). After ischemia/reperfusion, there was much more viable myocardium in KO hearts than WT hearts (red lesion (printed in black) in Fig. 4A). The infracted size was significantly smaller in KO hearts (32 ± 9%) than in WT hearts (68 ± 10%, $P<0.05$) (white lesion in Fig. 4A and Fig. 4B).

Concluding remarks

Myocardial cell injury is induced by a combination of mechanical and chemical stresses during ischemia

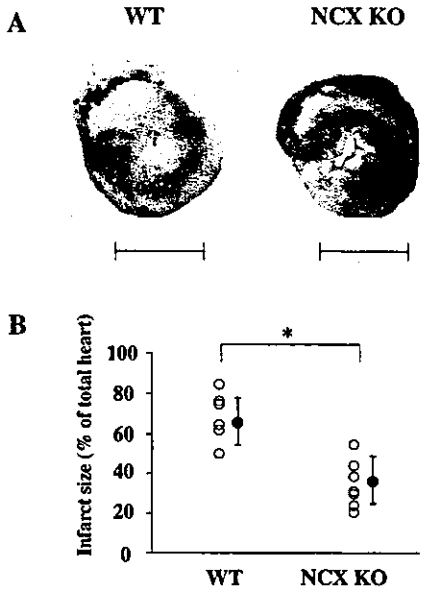

Fig. 4. Infarct size. A: Representative TTC staining photographs of WT and NCX KO mice hearts after ischemia/reperfusion are shown. Infarct area is expressed as a white lesion and viable myocardium is expressed as a red lesion (printed in black). Bar = 2 mm. B: Myocardial infarct size is expressed as percentage for the total heart of WT mice (n = 6) and NCX KO mice (n = 7). Values are expressed as the mean ± S.E.M. **P*<0.05 *vs* WT mice.

(14). Reoxygenation after extended periods of ischemia rapidly induce hypercontracture of cardiomyocytes (15) and aggravate the preexisting injury (16). The hypercontracture represents a major cause of acute lethal cell injury in the reperfused myocardium (17, 18). It has been hypothesized that an increase in intracellular Ca^{2+} levels of cardiomyocytes through NCX induces the hypercontracture state after reperfusion but not during ischemia by the mechanism described below (5). During myocardial ischemia, anaerobic metabolism induces acidosis both inside and outside of cardiomyocytes. The Na^+/H^+ exchanger does not operate at this moment because of no difference in H^+ concentration across the plasma membrane of cardiomyocytes. Reperfusion restores extracellular acidosis, leading to a disparity in H^+ concentration between the inside and outside of cardiomyocytes. The increase in intracellular H^+ concentration activates the Na^+/H^+ exchanger, and the elevated intracellular Na^+ concentration triggers a rise in intracellular Ca^{2+} by the reverse mode of NCX (5). The excessive Ca^{2+} overload induces the catastrophic hypercontracture of cardiomyocytes. In fact, it has been reported that reduction of Ca^{2+} concentration protects cardiomyocytes against hypercontracture evoked by reoxygenation (19). In contrast, overexpression of NCX

increased ischemia/reperfusion injury in mice (20). Pharmacological inhibition of reverse mode of NCX protected reperfusion injury in cardiomyocytes (19). These results suggest that NCX is critically involved in the myocardial ischemia/reperfusion injury; however, NCX inhibitors have been recently reported to be not specific to NCX (6). Two putative NCX inhibitors, KB-R7943 and SEA0400, depressed the Ca^{2+} transients even in cardiomyocytes of NCX null mice (7). Although these NCX inhibitors have been reported to suppress the reverse mode but not the forward mode of NCX, the administration of high dose of these inhibitors increased infarct size possibly by inhibiting the forward mode of NCX (21). We here demonstrated an important role of NCX in myocardial ischemia/reperfusion injury by using NCX KO mice. The reverse mode of NCX current in KO mice was decreased to half that of WT mice. Loss of function of NCX is assumed to result in alleviation of Ca^{2+} overload, hypercontracture, and cell death after reperfusion. Our present study clearly indicates that the inhibition of NCX contributes to cardioprotection against myocardial ischemia/reperfusion injury and suggests that specific inhibitors of the reverse mode of NCX may be useful to prevent the myocardial ischemia/reperfusion inury.

Acknowledgments

We thank to Y. Reien for the current density analysis and R. Kobayashi, E. Fujita, M. Watanabe, M. Iida, and A. Ohkubo for technical assistance. This work was supported in part by grants from the Japanese Ministry of Education, Culture, Sports, Science, and Technology and the Japan Health Sciences Foundation.

References

1 Schulze D, Kofuji P, Hadley R, Kirby MS, Kieval RS, Doering A, et al. Sodium/calcium exchanger in heart muscle: molecular biology, cellular function, and its special role in excitation-contraction coupling. Cardiovasc Res. 1993;27:1726–1734.

2 Bridge JH, Smolley JR, Spitzer KW. The relationship between charge movements associated with I_{Ca} and $I_{Na\text{-}Ca}$ in cardiac myocytes. Science. 1990;248:376–378.

3 Kleber AG. Resting membrane potential, extracellular potassium activity, and intracellular sodium activity during acute global ischemia in isolated perfused guinea pig hearts. Circ Res. 1983; 52:442–450.

4 Pilitsis JG, Diaz FG, O'Regan MH, Phillis JW. Inhibition of Na^+/Ca^{2+} exchange by KB-R7943, a novel selective antagonist, attenuates phosphoethanolamine and free fatty acid efflux in rat cerebral cortex during ischemia-reperfusion injury. Brain Res. 2001;916:192–198.

5 Eigel BN, Hadley RW. Antisense inhibition of Na^+/Ca^{2+} exchange during anoxia/reoxygenation in ventricular myocytes. Am J Physiol Heart Circ Physiol. 2001;281:H2184–H2190.

6 Reuter H, Henderson SA, Han T, Matsuda T, Baba A, Ross RS, et al. Knockout mice for pharmacological screening: testing the specificity of Na^+/Ca^{2+} exchange inhibitors. Circ Res. 2002; 91:90–92.

7 Wakimoto K, Kobayashi K, Kuro OM, Yao A, Iwamoto T, Yanaka N, et al. Targeted disruption of Na^+/Ca^{2+} exchanger gene leads to cardiomyocyte apoptosis and defects in heartbeat. J Biol Chem. 2000;275:36991–36998.

8 Suzuki M, Li RA, Miki T, Uemura H, Sakamoto N, Ohmoto-Sekine Y, et al. Functional roles of cardiac and vascular ATP-sensitive potassium channels clarified by Kir 6.2-knockout mice. Circ Res. 2001;88:570–577.

9 Watanabe Y, Kimura J. Inhibitory effect of amiodarone on Na^+/Ca^{2+} exchange current in guinea-pig cardiac myocytes. Br J Pharmacol. 2000;131:80–84.

10 Kimura J, Miyamae S, Noma A. Identification of sodium-calcium exchange current in single ventricular cells of guinea-pig. J Physiol (Lond). 1987;384:199–222.

11 Zou Y, Komuro I, Yamazaki T, Kudoh S, Uozumi H, Kadowaki T, et al. Both Gs and Gi proteins are critically involved in isoproterenolinduced cardiomyocyte hypertrophy. J Biol Chem. 1999;274:9760–9770.

12 Takimoto E, Yao A, Toko H, Takano H, Shimoyama M, Sonoda M, et al. Sodium calcium exchanger plays a key role in alteration of cardiac function in response to pressure overload. FASEB J. 2002;16:373–378.

13 Suzuki M, Sasaki N, Miki T, Sakamoto N, Ohmoto-Sekine Y, Tamagawa M, et al. Role of sarcolemmal K(ATP) channels in cardioprotection against ischemia/reperfusion injury in mice. J Clin Invest. 2002;109:509–516.

14 Piper HM, Garcia-Dorland D, Ovize M. A fresh look at reperfusion injury. Cardiovasc Res. 1998;38:291–300.

15 Siegmund B, Koop A, Klietz T, Schwartz P, Piper HM. Sarcolemmal integrity and metabolic competence of cardiomyocytes under anoxiareoxygenation. Am J Physiol. 1990;258: H285–H291.

16 Stern MD, Chien AM, Capogrossi MC, Pelto DJ, Lakatta EG. Direct observation of the "oxygen paradox" in single rat ventricular myocytes. Circ Res. 1985;56:899–903.

17 Barrabes JA, Garcia-Dorado D, Ruiz-Meana M, Piper HM, Solares J, Gonzalez MA, et al. Myocardial segment shrinkage during coronary reperfusion in situ. Relation to hypercontracture and myocardial necrosis. Pflugers Arch. 1996;431:519–526.

18 Ganote CE. Contraction band necrosis and irreversible myocardial injury. J Mol Cell Cardiol. 1983;15:67–73.

19 Schafer C, Ladilov Y, Inserte J, Schafer M, Haffner S, Garcia-Dorado D, et al. Role of the reverse mode of the Na^+/Ca^{2+} exchanger in reoxygenation-induced cardiomyocyte injury. Cardiovasc Res. 2001;51:241–250.

20 Cross HR, Lu L, Steenbergen C, Philipson KD, Murphy E. Overexpression of the cardiac Na^+/Ca^{2+} exchanger increases susceptibility to ischemia/reperfusion injury in male, but not female, transgenic mice. Circ Res. 1998;83:1215–1223.

21 Inserte J, Garcia-Dorado D, Ruiz-Meana M, Padilla F, Barrabes J, Pina P, et al. Effect of inhibition of Na^+/Ca^{2+} exchanger at the time of myocardial reperfusion on hypercontracture and cell death. Cardiovasc Res. 2002;55:739.

nature medicine

ARTICLES

Salt-sensitive hypertension is triggered by Ca^{2+} entry via Na^+/Ca^{2+} exchanger type-1 in vascular smooth muscle

Takahiro Iwamoto[1,3], Satomi Kita[1,5], Jin Zhang[2], Mordecai P Blaustein[2], Yuji Arai[4], Shigeru Yoshida[5], Koji Wakimoto[6], Issei Komuro[7] & Takeshi Katsuragi[1]

Excessive salt intake is a major risk factor for hypertension. Here we identify the role of Na^+/Ca^{2+} exchanger type 1 (NCX1) in salt-sensitive hypertension using SEA0400, a specific inhibitor of Ca^{2+} entry through NCX1, and genetically engineered mice. SEA0400 lowers arterial blood pressure in salt-dependent hypertensive rat models, but not in other types of hypertensive rats or in normotensive rats. Infusion of SEA0400 into the femoral artery in salt-dependent hypertensive rats increases arterial blood flow, indicating peripheral vasodilation. SEA0400 reverses ouabain-induced cytosolic Ca^{2+} elevation and vasoconstriction in arteries. Furthermore, heterozygous NCX1-deficient mice have low salt sensitivity, whereas transgenic mice that specifically express NCX1.3 in smooth muscle are hypersensitive to salt. SEA0400 lowers the blood pressure in salt-dependent hypertensive mice expressing NCX1.3, but not in SEA0400-insensitive NCX1.3 mutants. These findings indicate that salt-sensitive hypertension is triggered by Ca^{2+} entry through NCX1 in arterial smooth muscle and suggest that NCX1 inhibitors might be useful therapeutically.

Hypertension is the most common chronic disease, and is the leading risk factor for death that is due to stroke, myocardial infarction or end-stage renal failure[1,2]. The critical importance of excess salt intake in the pathogenesis of hypertension is widely recognized[3–6], but the mechanism by which excess salt intake elevates blood pressure has puzzled researchers. Recently discovered cardiotonic steroids (CTS), such as endogenous ouabain[7], and other steroids[8–10], including marinobufagenin, proscillaridin A and bufalin, have been proposed as candidate intermediaries. In humans, a chronic high-salt diet causes a rise in plasma CTS[11–13]. Moreover, ~50% of patients with essential hypertension have substantially elevated levels of endogenous ouabain[14,15]. Plasma CTS are also high in several salt-dependent hypertensive animals[7,13,16]. Indeed, PST2238, a ouabain antagonist, lowers blood pressure in salt-dependent hypertensive rats and in certain patients with essential hypertension[17,18]. Generally, it is believed that CTS inhibit the plasma membrane Na^+/K^+ ATPase, the 'sodium-potassium pump,' and lead to an increase in cytosolic Na^+ concentration ($[Na^+]_{cyt}$). Cellular Na^+ accumulation raises the cytosolic Ca^{2+} concentration ($[Ca^{2+}]_{cyt}$) through the involvement of the Na^+/Ca^{2+} exchanger (NCX), and thereby increases contraction in vascular or heart muscle. This may lead to hypertension[19], but the hypothesis has not yet been critically tested because little is understood of the function of NCX in these processes.

NCX is a plasma membrane transporter expressed in various cell types. Membrane potential and transmembrane gradients of Na^+ and Ca^{2+} control this bidirectional exchanger. The mammalian NCX family comprises three isoforms[20]. NCX1 is abundant in the heart, but is also expressed in many other tissues. In contrast, expression of NCX2 and NCX3 is restricted to brain and skeletal muscle. Extensive alternative splicing of NCX1 generates tissue-specific variants[21–23]; the heart expresses exclusively NCX1.1, and vascular tissue predominantly NCX1.3 and NCX1.7. Although the importance of this diversity is unclear, it may reflect different requirements for the maintenance of Ca^{2+} homeostasis in various cell types[20]. In cardiomyocytes, NCX1 has the primary role in Ca^{2+} extrusion during excitation-contraction coupling[24]. Under pathological conditions such as cardiac ischemia-reperfusion injury[25,26], NCX1 is thought to cause Ca^{2+} overload resulting from elevated $[Na^+]_{cyt}$; this leads to cardiac dysfunction. In other tissues, including vascular smooth muscle (VSM), NCX1 is also believed to extrude Ca^{2+} from the cytosol[25], but the physiological roles of vascular NCX1 are still unclear.

Recently, SEA0400, a specific NCX inhibitor that preferentially blocks the Ca^{2+} entry mode[27,28], was developed. We now report that SEA0400 lowers arterial blood pressure in salt- or ouabain-dependent hypertensive models, but not in normotensive rats or in other types of hypertensive rats. SEA0400 reverses the cytosolic Ca^{2+} elevation and vasoconstriction induced by nanomolar ouabain. Furthermore, we found that heterozygous mice with reduced expression of NCX1 resist development of salt-dependent hypertension. Conversely, transgenic mice with VSM-specific expression of NCX1 readily develop hypertension after high salt intake. These data provide compelling

[1]Department of Pharmacology, School of Medicine, Fukuoka University, Fukuoka 814-0180, Japan. [2]Department of Physiology, University of Maryland School of Medicine, Baltimore, Maryland 21201, USA. Departments of [3]Molecular Physiology and [4]Bioscience, National Cardiovascular Center Research Institute, Osaka 565-8565, Japan. [5]Medicinal Research Laboratories, Taisho Pharmaceutical Co., Ltd., Saitama 330-8530, Japan. [6]Discovery Research Laboratory, Tanabe Seiyaku Co., Ltd., Osaka 532-8505, Japan. [7]Department of Cardiovascular Science and Medicine, Chiba University Graduate School of Medicine, Chiba 260-8670, Japan. Correspondence should be addressed to T.I. (tiwamoto@cis.fukuoka-u.ac.jp).

Published online 10 October 2004; doi:10.1038/nm1118

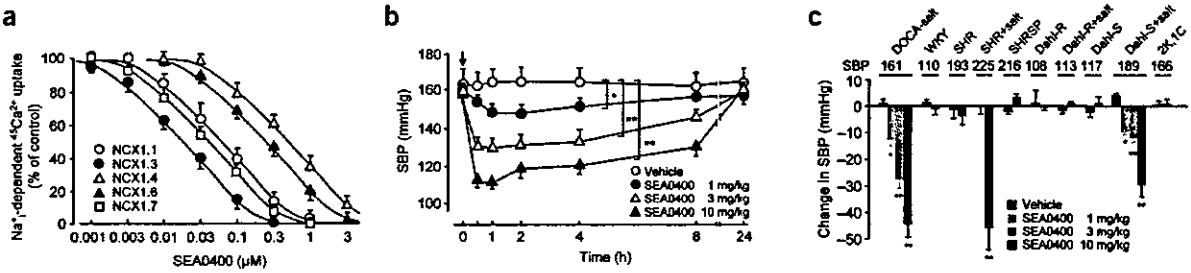

Figure 1 NCX1 inhibition and antihypertensive effects of SEA0400. (**a**) Concentration-response curves of SEA0400 for intracellular Na^+ (Na^+_i)-dependent $^{45}Ca^{2+}$ uptake into fibroblasts overexpressing variously spliced isoforms of human NCX1. Expression levels and NCX activities in these transfectants are shown in **Supplementary Figure 1** online. (**b**) Recordings over 24 h (9 a.m. to 9 a.m.) of SBP after oral administration of vehicle or SEA0400 (1–10 mg/kg) in DOCA-salt hypertensive rats. (**c**) Peak changes in SBP in various types of hypertensive rats treated with oral SEA0400. SHR, Dahl salt-resistant rats (Dahl-R) and Dahl salt-sensitive rats (Dahl-S) were fed a normal (0.3% NaCl) or high-salt diet (8% NaCl; +salt) for 4–6 weeks. Change in SBP in mmHg for the respective rats is indicated. Bars represent means ± s.e.m. ($n = 4$–6). WKY, Wistar Kyoto rats; SHRSP, stroke-prone SHR; 2K,1C, two-kidney, one-clip rats. $^*P < 0.05$, $^{**}P < 0.01$ compared with each vehicle group.

evidence that salt-dependent hypertension is triggered by Ca^{2+} entry through NCX1 in VSM cells. This finding also suggests that vascular NCX1 is a new therapeutic or diagnostic target for salt-sensitive hypertension.

RESULTS

Antihypertensive effects of SEA0400

In VSM cells, NCX1.3 and NCX1.7 are the dominant splicing isoforms[21–23]. By measuring intracellular Na^+-dependent Ca^{2+} uptake into fibroblasts overexpressing splicing isoforms of NCX1, we found that SEA0400, a specific inhibitor for Ca^{2+} entry through NCX1, preferentially blocks the vascular isoforms, especially NCX1.3 (**Fig. 1a** and **Supplementary Fig. 1** online). This finding indicates that SEA0400 is an excellent pharmacological tool for studying the vascular function of NCX1.

To evaluate the role of NCX1 in hypertension, we tested the effects of SEA0400 on various hypertensive models. A single oral dose of SEA0400 (1–10 mg/kg) caused a dose-dependent and long-lasting decrease in systolic blood pressure (SBP) in deoxycorticosterone acetate (DOCA)-salt hypertensive rats (**Fig. 1b**). Intravenous administration of SEA0400 (0.3–3 mg/kg) also lowered SBP in anesthetized DOCA-salt hypertensive rats (data not shown). Notably, however, SEA0400 did not significantly affect SBP in spontaneously hypertensive rats (SHR) or Wistar Kyoto rats ($P > 0.05$; **Fig. 1c**). We also examined the antihypertensive effect of SEA0400 in other hypertensive models. SEA0400 significantly decreased SBP in Dahl salt-sensitive rats and SHR when they were chronically loaded with high salt ($P < 0.01$; **Fig. 1c**). On the other hand, SEA0400 had no effect on SBP in stroke-prone SHR, salt-loaded or salt-unloaded Dahl salt-resistant rats, salt-unloaded Dahl salt-sensitive rats, or two-kidney, one-clip renal hypertensive rats. Thus, SEA0400 selectively suppresses salt-dependent hypertension.

The effect of chronic treatment with SEA0400 was also tested in DOCA-salt hypertensive rats. Administration of SEA0400 (3 or 10 mg/kg) for 3 weeks efficiently overcame the development of hypertension, vascular hypertrophy and renal dysfunction induced by DOCA-salt treatment (**Supplementary Fig. 2** and **Supplementary Tables 1 and 2** online). This suggests that SEA0400 has therapeutic potential as a new antihypertensive drug.

Direct vasodilation by SEA0400

To analyze its antihypertensive mechanism, we infused SEA0400 into the femoral artery of anesthetized DOCA-salt hypertensive rats (**Fig. 2a**). Intrafemoral infusion of SEA0400 (10 μg/kg/min) markedly increased femoral blood flow (FBF), indicating that SEA0400 caused peripheral vasodilation. A similar infusion did not affect FBF in normotensive sham rats. On the other hand, when the femoral artery of the sham rat (recipient) was crossperfused with aortic blood from the DOCA-salt hypertensive rat (donor), the intrafemoral infusion of SEA0400 significantly increased the FBF ($P < 0.05$; **Fig. 2b**). SEA0400 had no effect in the crossperfusion between two sham rats. This suggests that humoral vasoconstrictors participate in DOCA-salt hypertension; these vasoconstrictor effects can be antagonized by SEA0400.

Endogenous CTS are thought to contribute to the pathogenesis of salt-sensitive hypertension in patients and experimental animals[7,11–16]. Indeed, chronic administration of ouabain to rats causes hypertension[29,30]. Therefore, we examined the effect of SEA0400 on ouabain-induced hypertension. SEA0400 (1 or 10 mg/kg) suppressed hypertension in a dose-dependent manner in Sprague-Dawley rats on long-term ouabain treatment (**Fig. 3a**). SEA0400 did not affect the vasopressor responses to intravenous administration of norepinephrine, angiotensin II and endothelin-1 in anesthetized Sprague-Dawley rats (data not shown). Furthermore, to check the antagonistic interaction between ouabain and SEA0400, either ouabain or SEA0400, or both, were infused into the femoral arteries of anesthetized beagles. Intrafemoral infusion of SEA0400 (50 μg/kg/min) alone did not affect FBF. Infusion of either ouabain (0.5 μg/kg/min), however, reduced the FBF by approximately 50%; addition of SEA0400 then restored FBF to the basal level (**Fig. 3b**).

Effects of SEA0400 on pressurized small arteries

In VSM cells, inhibition of sarcolemmal Na^+/K^+ ATPases by endogenous CTS would be expected to increase $[Na^+]_{cyt}$ and subsequently to raise $[Ca^{2+}]_{cyt}$ through the NCX. To test this hypothesis, we examined the effects of low-dose ouabain and SEA0400 on $[Ca^{2+}]_{cyt}$ (measured as fluo-4 fluorescence) and vasoconstriction in intact, pressurized mouse small mesenteric arteries with myogenic tone. Ouabain (100 nM) increased fluo-4 fluorescence by ~12% and myogenic tone by 20–25% (**Fig. 4**). The physiological consequences of even small changes are profound because of Poiseuille's law[31]: resistance to blood flow, R, is inversely proportional to the fourth power of the internal radius, r ($R \propto 1/r^4$). Thus, a 5–10% rise in $[Ca^{2+}]_{cyt}$ should augment myogenic tone[32] enough to increase R (and blood pressure)[31] by ~20–50% (**Fig. 4**).

SEA0400 (300 nM) abolished the effects induced by low-dose ouabain. A video clip of the fluo-4 fluorescence data shown in

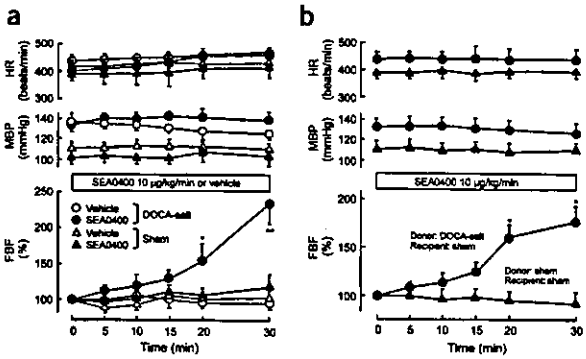

Figure 2 Vascular responses to intrafemoral infusion of SEA0400 in anesthetized DOCA-salt hypertensive or uninephrectomized sham rats. (**a**) SEA0400 or vehicle was infused at a rate of 20 μl/min into the femoral artery while monitoring the heart rate (HR), mean blood pressure (MBP), and femoral blood flow (FBF). (**b**) SEA0400 was infused into the femoral artery of the recipient (sham rat) crossperfused with the blood from the donor (DOCA-salt hypertensive rat or sham rat). Bars represent means ± s.e.m. ($n = 4$). $^*P < 0.05$; $^{**}P < 0.01$ compared with pretreatment values.

Figure 4b is available online as Supplementary Movie 1. In control arteries, SEA0400 also lowered $[Ca^{2+}]_{cyt}$ slightly (data not shown) and reduced normal myogenic tone by about 10% (Fig. 4c). SEA0400 had no effect on 75 mM K^+-induced vasoconstriction (data not shown), consistent with previous reports on SEA0400 selectivity[27,33]. These results suggest that the increased myogenic tone induced by low-dose ouabain, and even a part of the normal resting tone, may depend upon Ca^{2+} entry mediated by NCX.

Prevention of DOCA-salt hypertension in NCX1 heterozygous mice

To study the functional significance of NCX1 in salt-sensitive hypertension, the hypertensive responsiveness to DOCA-salt treatment was examined in heterozygous NCX1-deficient (*Slc8a1*$^{+/-}$) mice. The NCX1 protein level in the aorta, as well as in other organs[34], of *Slc8a1*$^{+/-}$ mice was about 50% of that seen in wild-type mice (Fig. 5). On the other hand, there were no differences in expression levels of Na^+/K^+-ATPase (α_2 and α_3), L-type Ca^{2+} channel (α_{1C}) and sarcolemmal Ca^{2+}-ATPase in aortas from *Slc8a1*$^{+/-}$ mice (data not shown). Basal SBP of *Slc8a1*$^{+/-}$ mice was no different from that of wild-type mice. DOCA-salt treatment produced a progressive elevation in SBP in wild-type mice ($P < 0.01$), whereas the same treatment did not significantly alter the SBP of *Slc8a1*$^{+/-}$ mice ($P > 0.05$; Fig. 5a). When the sodium level in drinking water for DOCA-salt treatment was increased from 1% to 2%, *Slc8a1*$^{+/-}$ mice responded with a mild increase in SBP (108 ± 3 mmHg ($n = 5$) at 3 weeks, $P < 0.05$), though wild-type mice experienced severe hypertension (128 ± 5 mmHg ($n = 5$), $P < 0.01$). In contrast, hypertensive responses to chronic angiotensin II infusion were similar in *Slc8a1*$^{+/-}$ and wild-type mice (Fig. 5b).

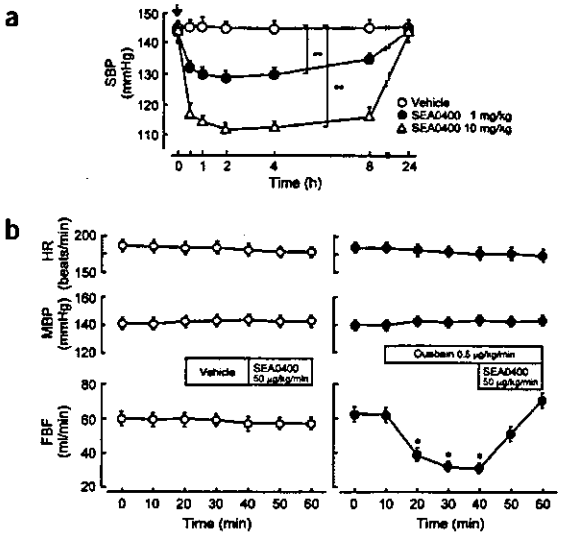

Salt hypersensitivity in VSM-specific NCX1.3 transgenic mice

To test further whether vascular NCX1 has a critical role in salt-sensitive hypertension, we created transgenic mice (*N1.3*$^{Tg/Tg}$) expressing canine *Ncx1.3* driven by the smooth muscle α-actin promoter (Fig. 6a). Southern blotting indicated that four founders had 2–4 copies of the transgene (data not shown). From among them, two independent transgenic lines were selected for detailed study. Western blot analysis showed that NCX1.3 protein was overexpressed in the aortas, but not in the hearts, of these transgenic mice at 6- to 8-fold the level of endogenous NCX1 (Supplementary Fig. 3 online). Immunohistochemical staining indicated dense localization of NCX1.3 in the medial layer of aortas from *N1.3*$^{Tg/Tg}$ mice (Fig. 6b). On the other hand, no difference was observed in protein levels of Na^+/K^+-ATPase (α_2 and α_3), L-type Ca^{2+} channel (α_{1C}) and sarcolemmal Ca^{2+} ATPase in aortas from *N1.3*$^{Tg/Tg}$ mice by western blotting (data not shown). Functional augmentation was correlated with increased NCX1 protein levels in aortas from *N1.3*$^{Tg/Tg}$ mice, as shown by measuring the rate and degree of contraction evoked by Na^+ removal in aortic rings pretreated with ouabain (Supplementary Fig. 3 online). Furthermore, the 10 μM ouabain-induced $[Ca^{2+}]_{cyt}$ rise in mesenteric arteries from *N1.3*$^{Tg/Tg}$ mice was notably greater than in those from wild-type mice (Fig. 6c,d).

Notably, the basal SBP of *N1.3*$^{Tg/Tg}$ mice (103 ± 1.4 mmHg, $n = 6$) was slightly, but significantly ($P < 0.05$), higher than that of wild-type mice (92 ± 1.1 mmHg, $n = 5$). When these mice were fed an 8% NaCl diet with 1% NaCl drinking water, SBP in *N1.3*$^{Tg/Tg}$ mice, but not in wild-type mice, progressively rose to 124 ± 3.5 mmHg ($n = 6$) at 4 weeks after the start of salt loading (Fig. 6e). Oral administration of SEA0400 (10 mg/kg) markedly lowered the SBP of salt-loaded *N1.3*$^{Tg/Tg}$ mice, but not of salt-loaded wild-type mice (Fig. 6f). Intravenous administration of SEA0400 (0.3 mg/kg) also lowered SBP in anesthetized *N1.3*$^{Tg/Tg}$ mice by about 20 mmHg (data not shown). In addition, oral administration of SEA0400 suppressed basal SBP (mild hypertension) of *N1.3*$^{Tg/Tg}$ mice, but not of wild-type mice, and abolished the difference between the two groups (Supplementary Fig. 3 online).

Figure 3 Effects of SEA0400 on ouabain-induced hypertension and vasoconstriction. (**a**) Recordings over 24 h of SBP after oral administration of SEA0400 in hypertensive rats infused subcutaneously with ouabain (30 μg/kg/d for 5 weeks). $^{**}P < 0.01$ compared with the vehicle group ($n = 5$). (**b**) Femoral blood flow (FBF) response to intrafemoral infusion of SEA0400 or vehicle at a rate of 0.2 ml/kg/min in the presence (right) or absence (left) of ouabain in anesthetized beagles. MBP and HR were monitored during the experimental periods. $^*P < 0.05$ compared with pretreatment values ($n = 4$).

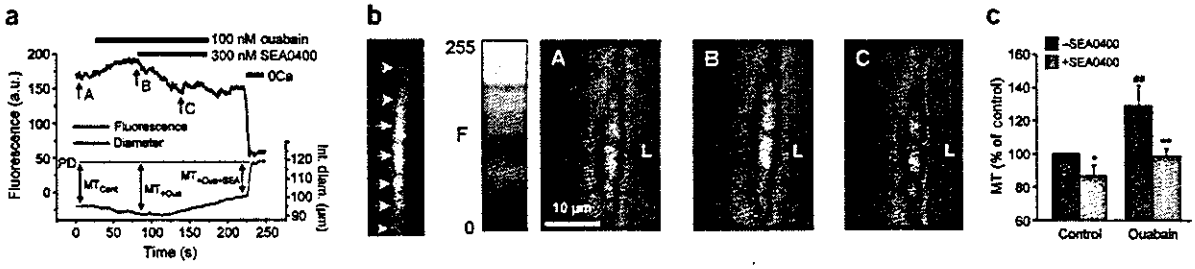

Figure 4 Effects of low-dose ouabain and SEA0400 on cytosolic Ca^{2+} level and myogenic tone (MT) in pressurized mouse small mesenteric arteries. (a) Simultaneous recording of fluorescence and internal diameter (Int. diam.) changes in a fluo-4 loaded artery (pressurized to 70 mmHg) by laser confocal microscopy. The fluo-4 fluorescence, indicated in arbitrary units (a.u.), reflects $[Ca^{2+}]_{cyt}$. Periods of exposure to ouabain, SEA0400 and Ca^{2+}-free medium (0Ca) are indicated by colored bars. The dotted line shows the passive internal diameter (PD) in 0Ca. (b) Fluorescent image on the left shows individual myocytes loaded with fluo-4 (arrows); the artery has only a single layer of myocytes. Pseudocolor images (**A–C**) indicate the relative $[Ca^{2+}]_{cyt}$ at the times shown in **a**. L, artery lumen. A video clip of the original data from this experiment is available at **Supplementary Movie 1** online. (c) Summary of the effects of ouabain and SEA0400 on MT, normalized to MT under control conditions. Mean PD was 107 ± 4 μm. At 70 mmHg, arteries constricted to 77 ± 4 μm internal diameter (= control MT). Ouabain caused a further constriction to 70 ± 4 μm; based on Poiseuille's law[31], this should increase resistance to blood flow (and blood pressure) by ~46%. $^{*}P < 0.05$; $^{**}P < 0.01$ versus pretreatment values ('–SEA0400'). $^{\#\#}P < 0.01$ versus control values ($n = 6$).

To verify that the antihypertensive effect of SEA0400 results from the inhibition of genetically overexpressed NCX1.3, we generated transgenic mice ($mN1.3^{Tg/Tg}$) expressing an SEA0400-insensitive G833C mutant[28] (Fig. 6a). Three independent lines of $mN1.3^{Tg/Tg}$ mice were selected for detailed analysis. The phenotypes of $mN1.3^{Tg/Tg}$ mice were very similar to those of $N1.3^{Tg/Tg}$ mice, except for their vascular response to SEA0400 (Fig. 6b–e and Supplementary Fig. 3 online); this drug blocked the contraction evoked by Na^+ removal in ouabain-pretreated aortic rings and the ouabain-induced $[Ca^{2+}]_{cyt}$ rise in arterial strips from $N1.3^{Tg/Tg}$ mice, but not from $mN1.3^{Tg/Tg}$ mice. In $mN1.3^{Tg/Tg}$ mice, SEA0400 (10 mg/kg) did not show a reduction in high salt–induced hypertension (Fig. 6f) and basal SBP (Supplementary Fig. 3 online). This shows that SEA0400 acts on the overexpressed NCX1.3 in VSM cells.

Given the possibility of nonspecific effects associated with NCX1 overexpression, as a further control we generated transgenic mice ($N1.1^{Tg/Tg}$) expressing canine *Ncx1.1* driven by the α-myosin heavy-chain promoter. In established $N1.1^{Tg/Tg}$ lines, hearts, but not aortas, showed a 2- to 3-fold increase in the level of NCX1 protein. Basal SBP of $N1.1^{Tg/Tg}$ mice was normal, and was similar to that of wild-type mice. Furthermore, the blood pressure of $N1.1^{Tg/Tg}$ mice, like that of wild-type mice, was resistant to long-term salt-loading and insensitive to the effect of SEA0400 (Supplementary Fig. 4 online).

DISCUSSION

The critical importance of sodium retention, resulting from excess salt intake or reduced renal salt excretion, in the pathogenesis of hypertension is widely recognized[3–6]. But the molecular mechanisms underlying salt-sensitive hypertension remain obscure. Here we show that SEA0400 lowers arterial blood pressure in various models of salt-dependent hypertension. SEA0400 does not, however, affect arterial blood pressure in normotensive rats or in other types of hypertensive rats. Furthermore, NCX1 heterozygous mice are resistant to DOCA-salt hypertension, but not to angiotensin II–induced hypertension. These findings suggest that vascular NCX1 is critical in the development of salt-sensitive hypertension.

The contraction of VSM cells is initiated by a rise in $[Ca^{2+}]_{cyt}$ through voltage-gated or receptor-operated Ca^{2+} channels in the sarcolemma, or both, or through Ca^{2+}-release channels in the sarcoplasmic reticulum membrane[35,36]. In general, sarcolemmal NCX, like the sarcolemmal or sarcoplasmic reticulum Ca^{2+}ATPases, is thought to contribute to Ca^{2+} extrusion from the cytosol in the relaxation process. Data obtained using antisense oligonucleotides indicate that NCX1 knockdown prolongs agonist responses by delaying the return of $[Ca^{2+}]_{cyt}$ to the resting level in cultured VSM cells[37,38].

To confirm the *in vivo* function of vascular NCX1 in mice, we generated VSM-specific transgenic mice expressing either wild-type NCX1.3 ($N1.3^{Tg/Tg}$) or the SEA0400-insensitive G833C mutant ($mN1.3^{Tg/Tg}$). Comparative experiments using these mutants and SEA0400 are useful for assessing the pharmacological significance of NCX inhibition[28]. Interestingly, both kinds of transgenic mice were mildly hypertensive (by about 10 mmHg) compared with wild-type mice. They also exhibited high salt–induced hypertension as a result of increased salt sensitivity. Administration of SEA0400 normalized

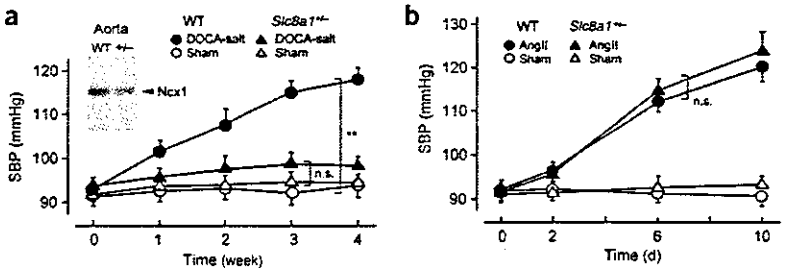

Figure 5 Prevention of DOCA-salt hypertension in $Slc8a1^{+/-}$ mice. (a) Uninephrectomized $Slc8a1^{+/-}$ and wild-type (WT) mice received DOCA (75 mg/kg) subcutaneously twice a week, and were given tap water containing 1% NaCl for 4 weeks. Sham mice were uninephrectomized but not given DOCA and salt. (b) Miniosmotic pumps containing angiotensin II (AngII) or vehicle (sham) were subcutaneously implanted in $Slc8a1^{+/-}$ and WT mice on day 0. Systolic blood pressure (SBP) was monitored by tail cuff. $^{**}P < 0.01$ versus control groups ($n = 5$ or 6).

blood pressure and suppressed salt-dependent hypertension in $N1.3^{Tg/Tg}$ mice, but not in $mN1.3^{Tg/Tg}$ mice. The latter mutation interferes with SEA0400 binding but does not affect Na^+/Ca^{2+} exchange[28]. In contrast, heart-specific transgenic mice expressing NCX1.1 were salt-insensitive, and their blood pressure did not respond to SEA0400. These results indicate that vascular NCX1 acts primarily as a Ca^{2+} entry pathway for regulating arterial tone, especially under sodium-retaining conditions. SEA0400 exerts its antihypertensive effect by blocking this Ca^{2+} entry in arterial myocytes.

Indeed, SEA0400 reverses the vasoconstriction and hypertension induced by exogenous ouabain, which may facilitate Ca^{2+} entry through NCX due to elevated $[Na^+]_{cyt}$, although SEA0400 does not directly affect the activity of Na^+/K^+-ATPases[27]. Notably, in VSM cells the NCX1 is colocalized with Na^+/K^+-ATPase α_2 and α_3 isoforms, which have high affinity for ouabain[39], in plasma membrane microdomains adjacent to the sarcoplasmic reticulum[40,41]. Functional coupling between NCX and Na^+/K^+-ATPase has been reported in vascular and cardiac myocytes[37,42–44]. As described above, endogenous plasma CTS are increased under pathological conditions such as salt-sensitive hypertension[7,11–16]. When CTS inhibit Na^+/K^+-ATPases (α_2 and α_3) in VSM cells, the elevation of local Na^+ in the submembrane area is expected to facilitate Ca^{2+} entry through NCX1, resulting in vasoconstriction. Our data indicate that blood from DOCA-salt hypertensive rats contains humoral vasoconstrictors whose action is counteracted by SEA0400. Also, using isolated, pressurized mouse small mesenteric arteries, we confirmed that 100 nM ouabain increases both $[Ca^{2+}]_{cyt}$ and myogenic tone by about 20–25% and that SEA0400 completely abolishes these effects. In addition, the 10 μM ouabain–induced $[Ca^{2+}]_{cyt}$ rise in arterial strips from transgenic mice was greater than in those from wild-type mice. SEA0400 blocked these $[Ca^{2+}]_{cyt}$ rises in $N1.3^{Tg/Tg}$ and wild-type mice, but not in $mN1.3^{Tg/Tg}$ mice. These data provide evidence that ouabain triggers Ca^{2+} entry through NCX1 in VSM cells by inhibiting high ouabain–affinity Na^+ pumps (α_2 or α_3) and elevating submembrane Na^+. Although ouabain has also been reported to mediate other signaling pathways[45], they apparently are not involved in the VSM mechanism described here.

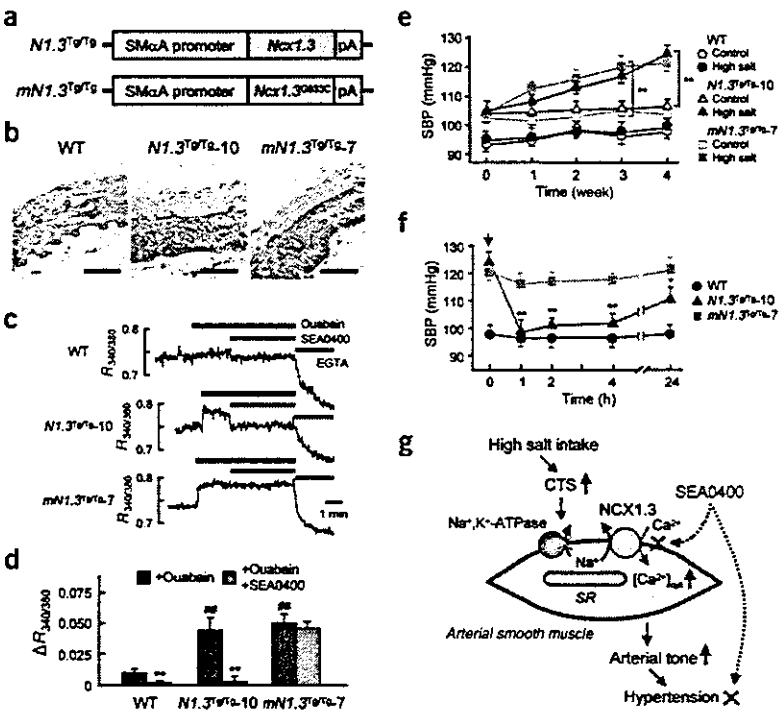

Figure 6 Enhanced salt-sensitivity in $N1.3^{Tg/Tg}$ or $mN1.3^{Tg/Tg}$ mice. (a) Schematic representation of the transgene used to generate VSM-specific transgenic mice. The *Ncx1.3* or its G833C mutant ($Ncx1.3^{G833C}$) was brought under the control of human smooth muscle α-actin (SMαA) promoter. (b) Immunohistochemical localization of NCX1 proteins in the medial layer of thoracic aortas from wild-type (WT) mice and two representative transgenic lines ($N1.3^{Tg/Tg}$-10 and $mN1.3^{Tg/Tg}$-7). Scale bars, 50 μm. (c) Effects of ouabain and SEA0400 on $[Ca^{2+}]_{cyt}$ (fura-PE3 fluorescence ratio ($R_{340/380}$)) in isolated mesenteric arteries from transgenic and WT mice. Periods of exposure to 10 μM ouabain, 1 μM SEA0400 and 4 mM EGTA are indicated by bars. All experiments were performed in the presence of 10 μM nicardipine to suppress L-type Ca^{2+} channels. (d) Summary of the experiments shown in (c). $^{**}P < 0.01$ versus pretreatment values ('+Ouabain'). $^{\#\#}P < 0.01$ versus WT groups ($n = 5$). (e,f) Salt-induced hypertension and antihypertensive effects of SEA0400 (10 mg/kg) in transgenic and WT mice treated with a high-salt diet (8% NaCl) and tap water containing 1% NaCl for 4 weeks. $^{*}P < 0.05$; $^{**}P < 0.01$ ($n = 5$ or 6). (g) Proposed pathway responsible for salt-sensitive hypertension. High salt intake causes the levels of endogenous CTS to rise in the plasma. This results in the increase in subplasma membrane $[Na^+]$ of arterial smooth muscle. The restricted $[Na^+]$ accumulation elevates $[Ca^{2+}]_{cyt}$ by vascular NCX1 isoform–mediated Ca^{2+} entry. This enhances arterial tone and causes hypertension. SEA0400 blocks this Ca^{2+} entry and exerts an antihypertensive effect in salt-sensitive hypertension.

SEA0400 does not affect arterial blood pressure in normotensive or salt-independent hypertensive animals. Intrafemoral infusion of SEA0400 in normal rats and beagles does not change arterial blood flow unless the arteries are perfused with exogenous ouabain or aortic blood from salt-dependent hypertensive animals. In addition, NCX1 heterozygous mice maintain normal blood pressure. Thus, the Ca^{2+} entry mode of NCX1 in VSM cells apparently has little role in blood pressure control in normotensive or in salt-insensitive hypertensive animals, probably owing to low plasma levels of CTS and to the overriding effects of reflex regulatory mechanisms. Nevertheless, the Ca^{2+} entry mode of NCX1 could have a role in regional blood flow even in normotensive and salt-insensitive animals, because SEA0400 slightly suppresses basal myogenic tone with a small reduction of $[Ca^{2+}]_{cyt}$ in pressurized mouse small mesenteric arteries.

In conclusion, our results show that the Ca^{2+} entry mode of vascular NCX1 is involved in the contractile regulation of small arteries and in the development of salt-dependent hypertension. Notably, recent human genome–wide linkage analysis of genes that affect blood pressure identified four regions, one of which includes *SLC8A1*, as loci containing candidate genes that influence blood pressure[46]. In humans and animals, endogenous CTS levels increase in plasma during salt retention[7,11–16]. Inhibition of Na^+ pumps by CTS should elevate local Na^+ and, through NCX1, $[Ca^{2+}]_{cyt}$ in VSM cells, thereby

promoting vasoconstriction (Fig. 6g). In this pathway, vascular NCX1 is a key mediator. SEA0400 selectively blocks NCX1.3, the vascular isoform of NCX1, and suppresses salt-dependent hypertension and associated secondary organ damage. Thus, the Ca^{2+} entry mode of vascular NCX1 may be a useful target for the development of therapies for salt-sensitive hypertension. Indeed, response to inhibitors of NCX1 may be diagnostic for salt-sensitive hypertension and involvement of the pathway illustrated in Figure 6g.

METHODS

$^{45}Ca^{2+}$ uptake. To examine the splice isoform selectivity of SEA0400, we cloned *NCX1.1*, *NCX1.3*, *NCX1.4*, *NCX1.6* and *NCX1.7* into pcDNA3.1 (Invitrogen) by PCR using human aortic cDNAs (Clontech). We transfected these plasmids with Lipofectin (Invitrogen) into CCL39 fibroblasts and we selected cells stably expressing NCX1 using a Ca^{2+}-killing procedure[47]. Intracellular Na^+-dependent $^{45}Ca^{2+}$ uptake into cells was assayed as described[47] (see Supplementary Methods online).

Experimental hypertensive models. To produce DOCA-salt hypertensive animals, 5-week-old male Sprague-Dawley rats or 12-week-old male mice were unilaterally nephrectomized under anesthesia with sodium pentobarbital. After allowing the animals a 1-week recovery, we administered DOCA (15 mg/kg for rats or 75 mg/kg for mice) with corn oil subcutaneously twice a week for 4 weeks. These animals then drank tap water containing 1% NaCl. Control animals (sham) were uninephrectomized but not given DOCA and salt. In the preparation of two-kidney, one-clip renal hypertensive rats, we anesthetized male Sprague-Dawley rats with sodium pentobarbital, and partially occluded the left renal artery by a silver clip (0.2 mm in diameter) for 4 weeks. To produce ouabain-induced hypertension, we infused ouabain subcutaneously at a rate of 30 μg/kg/day into male Sprague-Dawley rats by miniosmotic pumps (ALZET 2002) for 5 weeks. Ouabain was dissolved in sterile phosphate-buffered saline. To produce angiotensin II–induced hypertension, we subcutaneously implanted miniosmotic pumps containing either vehicle (0.01 N acetic acid in saline solution) or angiotensin II (750 μg/kg/d for 10 d) in male mice. We measured SBP at room temperature by a tail cuff method using an MK2000 blood pressure monitor (Muromachi Kikai). Rats or mice were acclimated to the procedures of blood pressure measurement for a week preceding actual data collection. We administered SEA0400 orally or intravenously with 5% gum arabic or a lipid emulsion containing 20% soybean oil (vehicle), respectively.

Intrafemoral infusion. To determine the peripheral vasodilation, we infused SEA0400 (10 μg/kg/min) or vehicle at a rate of 20 μl/min through a polyethylene tube in the right femoral artery of DOCA-salt hypertensive rats or uninephrectomized sham rats, anesthetized with sodium pentobarbital. In other experiments, we infused SEA0400 into the right femoral artery of the sham rat (recipient), which was crossperfused with vena caval and aortic blood of the donor rat and stabilized for 30 min. In yet other experiments, we infused SEA0400 (50 μg/kg/min) alone or in combination with ouabain (0.5 μg/kg/min) at a rate of 0.2 ml/min into the left femoral artery of anesthetized male beagles (9–10 kg). In all these experiments, FBF, systemic blood pressure and heart rate were monitored directly with a square-wave flowmeter and a pressure transducer (Nihon Koden), respectively.

Transgenic mice. We constructed the transgene by inserting canine *Ncx1.3* or its G833C mutant[28] between the human smooth muscle α-actin promoter and the SV40 polyadenylation sequence of the plasmid (T. Miwa). We also prepared an additional transgene by inserting canine *Ncx1.1* between the mouse α-myosin heavy chain promoter and the SV40 polyadenylation sequence of the plasmid (J. Robbins). Each transgene was microinjected into the pronuclei of fertilized C57BL/6J mouse embryos at the single-cell stage. We implanted the embryos into pseudopregnant foster mothers. Positive transgenic mice were identified as described[34]; mice were bred to homozygosity.

Imaging of small mesenteric arteries. Diameter measurement and Ca^{2+} imaging of mouse mesenteric artery were performed as described[48]. Distal mesenteric arteries (2–3 mm length, 120–150 μm passive external diameter) from male C57BL/6J mice were cannulated at both ends and continuously superfused with gassed Krebs solution (37 °C, 70 mmHg) to induce myogenic tone. For measurement of diameter only, the artery outer diameter was continuously monitored by a real-time edge-detection system (National Instruments). For Ca^{2+} imaging, arterial segments were loaded with 15 μM fluo-4-AM for ~3 h. We imaged dye-loaded arteries with a confocal imaging system (Nipkow-Yokogawa dual spinning disk, Solamere Technology) connected to a Nikon Eclipse 2000 microscope equipped with a water immersion objective (×60). Images were captured at the rate of 2–4 frames/s.

Other procedures and materials. Immunoblotting for membrane proteins and immunohistochemistry of frozen sections were performed as described[47,49], with some modifications. We performed analyses of aortic morphology and renal function as described[50]. We also performed measurements of contraction in aortic rings and $[Ca^{2+}]_{cyt}$ (fura-PE3 fluorescence ratio; $R_{340/380}$) in arterial strips as described[34,38], with some modifications (see Supplementary Methods online). We used an unpaired *t*-test, one-way ANOVA followed by Dunnett's test or two-way ANOVA for statistical analyses. Values of $P < 0.05$ were considered statistically significant. SEA0400 (2-[4-[(2,5-difluorophenyl)methoxy]phenoxy]-5-ethoxyaniline) was synthesized by Taisho Pharmaceutical Co. Ltd.

Animal regulations. We used all animals in accordance with the Guidelines for Animal Experiments in Fukuoka University and the US National Institutes of Health Guide for the Care and Use of Laboratory Animals.

Note: Supplementary information is available on the Nature Medicine website.

ACKNOWLEDGMENTS

We thank K. Takahashi and S. Okuyama (Taisho Pharmaceutical Co. Ltd.), K. Saku and H. Urata (Fukuoka University), J. Kimura (Fukushima Medical University) and Y. Matsumura (Osaka University of Pharmaceutical Sciences) for discussions, and W.G. Wier and R. Saunders (University of Maryland) for help in making the video clip. This work was supported by Grants-in-Aid for scientific research (14570097, 16590213) from the Ministry of Education, Science and Culture of Japan, a grant from the Salt Science Research Foundation (No.02), US National Institutes of Health grant HL-45215, and an American Heart Association Mid-Atlantic Affiliate Postdoctoral Fellowship.

COMPETING INTERESTS STATEMENT

The authors declare that they have no competing financial interests.

Received 20 May; accepted 8 September 2004
Published online at http://www.nature.com/naturemedicine/

1. Mosterd, A. *et al.* Trends in the prevalence of hypertension, antihypertensive therapy, and left ventricular hypertrophy from 1950 to 1989. *N. Engl. J. Med.* **340**, 1221–1227 (1999).
2. Kannel, W.B. Elevated systolic blood pressure as a cardiovascular risk factor. *Am. J. Cardiol.* **85**, 251–255 (2000).
3. Cowley, A.W. Long-term control of arterial blood pressure. *Physiol. Rev.* **72**, 231–300 (1992).
4. Blaustein, M.P. Physiological effects of endogenous ouabain: control of intracellular calcium stores and cell responsiveness. *Am. J. Physiol.* **264**, C1367–C1387 (1993).
5. Haddy, F.J. & Pamnani, M.B. Role of dietary salt in hypertension. *J. Am. Coll. Nutr.* **14**, 428–438 (1995).
6. Lifton, R.P., Gharavi, A.G. & Geller, D.S. Molecular mechanisms of human hypertension. *Cell* **104**, 545–556 (2001).
7. Hamlyn, J.M. *et al.* Identification and characterization of a ouabain-like compound from human plasma. *Proc. Natl. Acad. Sci. USA* **88**, 6259–6263 (1991).
8. Schneider, R. *et al.* Bovine adrenals contain, in addition to ouabain, a second inhibitor of the sodium pump. *J. Biol. Chem.* **273**, 784–792 (1998).
9. Bagrov, A.Y. *et al.* Characterization of a urinary bufodienolide Na^+,K^+-ATPase inhibitor in patients after acute myocardial infarction. *Hypertension* **31**, 1097–1103 (1998).
10. Schoner, W. Endogenous cardiac glycosides, a new class of steroid hormones. *Eur. J. Biochem.* **269**, 2440–2448 (2002).
11. Hamlyn, J.M. *et al.* A circulating inhibitor of (Na^++K^+)-ATPase associated with essential hypertension. *Nature* **300**, 650–652 (1982).
12. Hasegawa, T., Masugi, F., Ogihara, T. & Kumahara, Y. Increase in plasma ouabain-like inhibitor of Na^+,K^+-ATPase with high sodium intake in patients with essential hypertension. *J. Clin. Hypertens.* **3**, 419–429 (1987).
13. Hamlyn, J.M., Hamilton, B.P. & Manunta, P. Endogenous ouabain, sodium balance and blood pressure: a review and a hypothesis. *J. Hypertens.* **14**, 151–167 (1996).

14. Manunta, P. *et al.* Left ventricular mass, stroke volume, and ouabain-like factor in essential hypertension. *Hypertension* **34**, 450–456 (1999).
15. Goto, A. & Yamada, K. Putative roles of ouabainlike compound in hypertension: revisited. *Hypertens. Res.* **23**, S7–S13. (2000).
16. Fedorova, O.V., Lakatta, E.G. & Bagrov, A.Y. Endogenous Na,K pump ligands are differentially regulated during acute NaCl loading of Dahl rats. *Circulation* **102**, 3009–3014 (2000).
17. Ferrari, P. *et al.* PST2238: a new antihypertensive compound that antagonizes the long-term pressor effect of ouabain. *J. Pharmacol. Exp. Ther.* **285**, 83–94 (1998).
18. Takahashi, H. Endogenous digitalislike factor: an update. *Hypertens. Res.* **23**, S1–S5 (2000).
19. Blaustein, M.P. Sodium ions, calcium ions, blood pressure regulation, and hypertension: a reassessment and a hypothesis. *Am. J. Physiol.* **232**, C165–C173 (1977).
20. Philipson, K.D. & Nicoll, D.A. Sodium-calcium exchange: a molecular perspective. *Annu. Rev. Physiol.* **62**, 111–133. (2000).
21. Nakasaki, Y., Iwamoto, T., Hanada, H., Imagawa, T. & Shigekawa, M. Cloning of the rat aortic smooth muscle Na^+/Ca^{2+} exchanger and tissue-specific expression of isoforms. *J. Biochem.* **114**, 528–534 (1993).
22. Lee, S.L., Yu, A.S. & Lytton, J. Tissue-specific expression of Na^+-Ca^{2+} exchanger isoforms. *J. Biol. Chem.* **269**, 14849–14852 (1994).
23. Quednau, B.D., Nicoll, D.A. & Philipson, K.D. Tissue specificity and alternative splicing of the Na^+/Ca^{2+} exchanger isoforms NCX1, NCX2, and NCX3 in rat. *Am. J. Physiol.* **272**, C1250–C1261 (1997).
24. Bers, D.M. Cardiac excitation-contraction coupling. *Nature* **415**, 198–205 (2002).
25. Blaustein, M.P. & Lederer, W.J. Sodium/calcium exchange: its physiological implications. *Physiol. Rev.* **79**, 763–854 (1999).
26. Shigekawa, M. & Iwamoto, T. Cardiac Na^+-Ca^{2+} exchange: molecular and pharmacological aspects. *Circ. Res.* **88**, 864–876 (2001).
27. Matsuda, T. *et al.* SEA0400, a novel and selective inhibitor of the Na^+-Ca^{2+} exchanger, attenuates reperfusion injury in the in vitro and in vivo cerebral ischemic models. *J. Pharmacol. Exp. Ther.* **298**, 249–256 (2001).
28. Iwamoto, T. *et al.* Molecular determinants of Na^+/Ca^{2+} exchange (NCX1) inhibition by SEA0400. *J. Biol. Chem.* **279**, 7544–7553 (2004).
29. Yuan, C.M. *et al.* Long-term ouabain administration produces hypertension in rats. *Hypertension* **22**, 178–187 (1993).
30. Manunta, P., Rogowski, A.C., Hamilton, B.P. & Hamlyn, J.M. Ouabain-induced hypertension in the rat: relationships among plasma and tissue ouabain and blood pressure. *J. Hypertens.* **12**, 549–560 (1994).
31. Berne, R.M. & Levy, M.N. Chapter V. Hemodynamics. in *Cardiovascular Physiology* edn. 8 (eds. Berne, R.M. & Levy, M.N.) 115–134 (Mosby, St. Louis, 2001).
32. Knot, H.J. & Nelson, M.T. Regulation of arterial diameter and wall $[Ca^{2+}]$ in cerebral arteries of rat by membrane potential and intravascular pressure. *J. Physiol.* **508**, 199–209 (1998).
33. Tanaka, H. *et al.* Effect of SEA0400, a novel inhibitor of sodium-calcium exchanger, on myocardial ionic currents. *Br. J. Pharmacol.* **135**, 1096–1100 (2002).
34. Wakimoto, K. *et al.* Targeted disruption of Na^+/Ca^{2+} exchanger gene leads to cardiomyocyte apoptosis and defects in heartbeat. *J. Biol. Chem.* **275**, 36991–36998 (2000).
35. Berridge, M.J., Bootman, M.D. & Roderick, H.L. Calcium signalling: dynamics, homeostasis and remodelling. *Nat. Rev. Mol. Cell Biol.* **4**, 517–529 (2003).
36. Poburko, D., Kuo, K.H., Dai, J., Lee, C.H. & van Breemen, C. Organellar junctions promote targeted Ca^{2+} signaling in smooth muscle: why two membranes are better than one. *Trends Pharmacol. Sci.* **25**, 8–15 (2004).
37. Slodzinski, M.K., Juhaszova, M. & Blaustein, M.P. Antisense inhibition of Na^+/Ca^{2+} exchange in primary cultured arterial myocytes. *Am. J. Physiol.* **269**, C1340–C1345 (1995).
38. Slodzinski, M.K. & Blaustein, M.P. Physiological effects of Na^+/Ca^{2+} exchanger knockdown by antisense oligodeoxynucleotides in arterial myocytes. *Am. J. Physiol.* **275**, C251–C259 (1998).
39. Sweadner, K.J. Isozymes of the Na^+/K^+-ATPase. *Biochim. Biophys. Acta.* **988**, 185–220 (1989).
40. Moore, E.D. *et al.* Coupling of the Na^+/Ca^{2+} exchanger, Na^+/K^+ pump and sarcoplasmic reticulum in smooth muscle. *Nature* **365**, 657–660 (1993).
41. Juhaszova, M. & Blaustein, M.P. Distinct distribution of different Na^+ pump α subunit isoforms in plasmalemma. Physiological implications. *Ann. N.Y. Acad. Sci.* **834**, 524–536 (1997).
42. Fujioka, Y., Matsuoka, S., Ban, T. & Noma, A. Interaction of the Na^+-K^+ pump and Na^+-Ca^{2+} exchange via $[Na^+]_i$ in a restricted space of guinea-pig ventricular cells. *J. Physiol.* **509**, 457–470 (1998).
43. Arnon, A., Hamlyn, J.M. & Blaustein, M.P. Ouabain augments Ca^{2+} transients in arterial smooth muscle without raising cytosolic Na^+. *Am. J. Physiol.* **279**, H679–H691 (2000).
44. Reuter, H. *et al.* The Na^+-Ca^{2+} exchanger is essential for the action of cardiac glycosides. *Circ. Res.* **90**, 305–308 (2002).
45. Aizman, O., Uhlen, P., Lal, M., Brismar, H. & Aperia, A. Ouabain, a steroid hormone that signals with slow calcium oscillations. *Proc. Natl. Acad. Sci. USA* **98**, 13420–13424 (2001).
46. Krushkal, J. *et al.* Genome-wide linkage analyses of systolic blood pressure using highly discordant siblings. *Circulation* **99**, 1407–1410 (1999).
47. Iwamoto, T., Pan, Y., Nakamura, T.Y., Wakabayashi, S. & Shigekawa, M. Protein kinase C-dependent regulation of Na^+/Ca^{2+} exchanger isoforms NCX1 and NCX3 does not require their direct phosphorylation. *Biochemistry* **37**, 17230–17238 (1998).
48. Zhang, J., Wier, W.G. & Blaustein, M.P. Mg^{2+} blocks myogenic tone but not K^+-induced constriction: role for SOCs in small arteries. *Am. J. Physiol.* **283**, H2692–H2705 (2002).
49. Yamashita, J. *et al.* Attenuation of ischemia/reperfusion-induced renal injury in mice deficient in Na^+/Ca^{2+} exchanger. *J. Pharmacol. Exp. Ther.* **304**, 284–293 (2003).
50. Matsumura, Y. *et al.* Exaggerated vascular and renal pathology in endothelin-B receptor-deficient rats with deoxycorticosterone acetate-salt hypertension. *Circulation* **102**, 2765–2773 (2000).

THE JOURNAL OF CELL BIOLOGY

Cardiomyocytes fuse with surrounding noncardiomyocytes and reenter the cell cycle

Katsuhisa Matsuura,[1,2] Hiroshi Wada,[1] Toshio Nagai,[1] Yoshihiro Iijima,[1] Tohru Minamino,[1] Masanori Sano,[1] Hiroshi Akazawa,[1] Jeffery D. Molkentin,[3] Hiroshi Kasanuki,[2] and Issei Komuro[1]

[1]Department of Cardiovascular Science and Medicine, Chiba University Graduate School of Medicine, Chiba 260-8670, Japan
[2]Department of Cardiology, The Heart Institute of Japan, Tokyo Women's Medical University, Tokyo 162-8666, Japan
[3]Division of Molecular Cardiovascular Biology, Department of Pediatrics, Cincinnati Children's Hospital Medical Center, Cincinnati, OH 45229

The concept of the plasticity or transdifferentiation of adult stem cells has been challenged by the phenomenon of cell fusion. In this work, we examined whether neonatal cardiomyocytes fuse with various somatic cells including endothelial cells, cardiac fibroblasts, bone marrow cells, and endothelial progenitor cells spontaneously in vitro. When cardiomyocytes were cocultured with endothelial cells or cardiac fibroblasts, they fused and showed phenotypes of cardiomyocytes. Furthermore, cardiomyocytes reentered the G2-M phase in the cell cycle after fusing with proliferative noncardiomyocytes. Transplanted endothelial cells or skeletal muscle–derived cells fused with adult cardiomyocytes in vivo. In the cryo-injured heart, there were Ki67-positive cells that expressed both cardiac and endothelial lineage marker proteins. These results suggest that cardiomyocytes fuse with other cells and enter the cell cycle by maintaining their phenotypes.

Introduction

Many reports have indicated that adult stem cells have "plasticity" and transdifferentiate into various types of cells including cardiomyocytes (Jackson et al., 2001; Orlic et al., 2001a; Badorff et al., 2003). Bone marrow cells have been incorporated into the damaged myocardium and have expressed cardiac-specific proteins (Jackson et al., 2001; Orlic et al., 2001a; Mangi et al., 2003). Besides undifferentiated stem cells, differentiated somatic cells such as endothelial cells and skeletal muscle–derived cells have been also reported to transdifferentiate into cardiomyocytes when cocultured with cardiomyocytes (Condorelli et al., 2001; Iijima et al., 2003). However, the concept of plasticity has been challenged by the new findings that embryonic stem cells adopt the phenotype of bone marrow cells or central nervous stem cells by cell fusion (Terada et al., 2002; Ying et al., 2002). Bone marrow cells have been reported to fuse with hepatocytes in the severely injured liver and proliferate extensively, resulting in millions of highly aneuploid new hepatocytes (Vassilopoulos et al., 2003; Wang et al., 2003). In the brain, bone marrow cells form stable heterokaryons with Purkinje neurons in the absence of selective pressure. In this intracellular milieu, bone marrow cell–derived nuclei are reprogrammed to activate the Purkinje-specific gene, resulting in the phenotype of the Purkinje cells becoming dominant over time (Weimann et al., 2003). These results suggest that cell fusion might be one of the physiological mechanisms through which the cells change their lineage and the tissues are rejuvenated or regenerated.

Adult cardiomyocytes have been thought to be terminally differentiated and unable to divide, thus myocyte growth under pathologic conditions as well as physiologic conditions is believed to be accomplished only by cellular hypertrophy (Morgan and Baker, 1991; Chien, 1995). Cytoplasmic extracts of adult cardiomyocytes have been reported to reduce the expression of proliferating cell nuclear antigens in proliferating noncardiomyocytes (Engel et al., 2003), suggesting that some inhibitory molecules of the cell cycle might exist in the cytoplasm of adult cardiomyocytes. However, recent reports have indicated that adult cardiomyocytes can divide after myocardial infarction and at end-stage heart failure (Kajstura et al., 1998; Beltrami et al., 2001). The precise mechanism of how cardiomyocytes acquire proliferative ability is still elusive, but there is a possibility that mobilized bone marrow–derived stem cells or cardiac progenitor cells start to proliferate in response to some environmental cues (Orlic et al., 2001b; Beltrami et al.,

K. Matsuura and H. Wada contributed equally to this paper.

The online version of this article includes supplemental material.

Correspondence to Issei Komuro: komuro-tky@umin.ac.jp

Abbreviations used in this paper: ANF, atrial natriuretic factor; β-gal, β-galactosidase; CAT, chloramphenicol acetyltransferase; cFB, cardiac fibroblasts; cTnT, cardiac troponin T; EPC, endothelial progenitor cell; HUVEC, human umbilical vein endothelial cells; PH3, phosphohistone H3; RFP, red fluorescent protein; UEA-1, ulex europaeus agglutinin-1; vWF, von Willebrand factor.

The Rockefeller University Press $8.00
The Journal of Cell Biology, Vol. 167, No. 2, October 25, 2004 351–363
http://www.jcb.org/cgi/doi/10.1083/jcb.200312111

Supplemental Material can be found at:
http://www.jcb.org/cgi/content/full/jcb.200312111/DC1

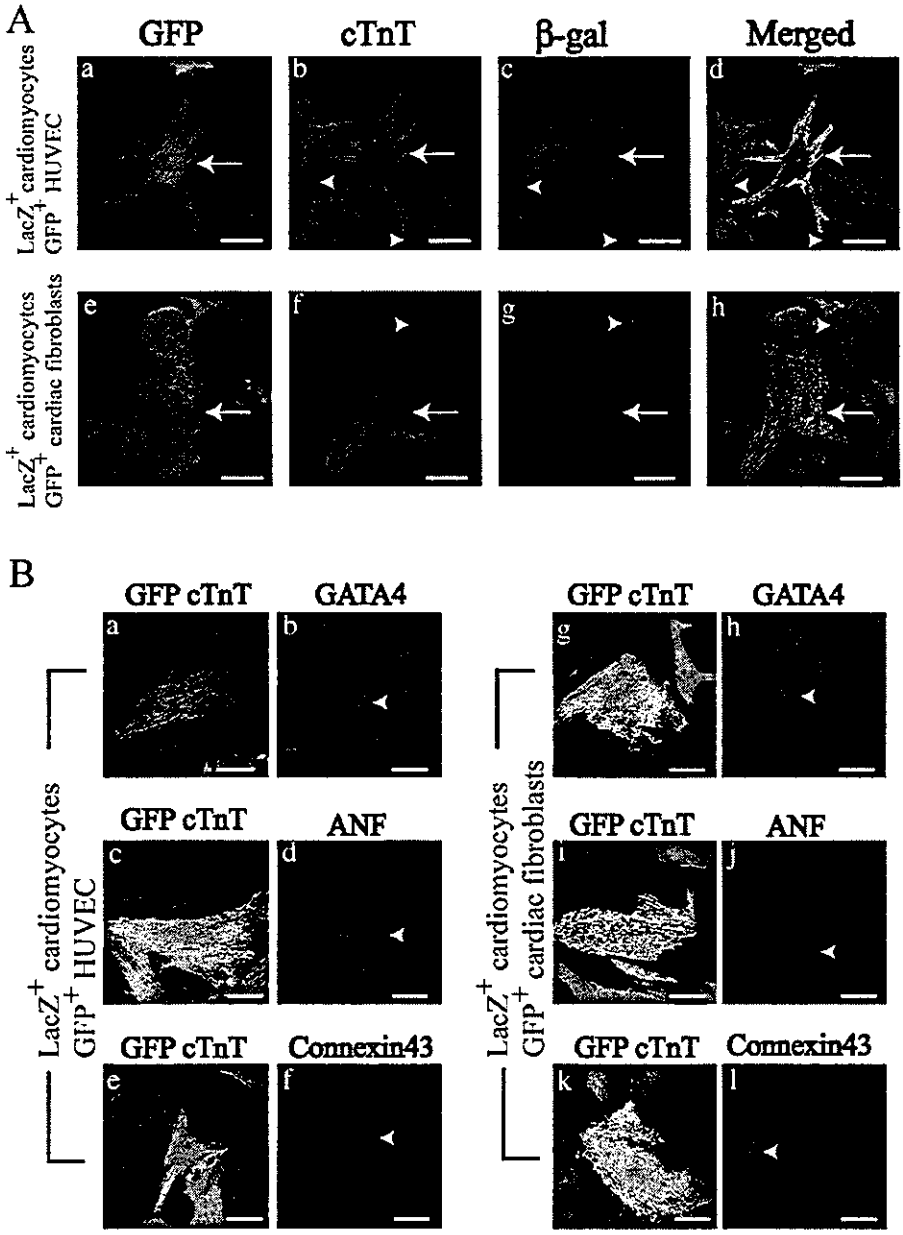

Figure 1. **HUVEC and cFB acquired the cardiac phenotype through cell fusion with cardiomyocytes.** (A) *LacZ*-expressing cardiomyocytes of neonatal rats were cocultured with GFP+ HUVEC (a–d) or GFP+ cFB (e–h) and stained with mouse monoclonal anti-cTnT (red) and rabbit polyclonal anti-β-gal antibodies (blue). Merged images were obtained from the same confocal plane. GFP+ HUVEC and GFP+ cFB (a and e, arrow) expressed cTnT (b and f, arrow) and β-gal (c and g, arrow) in the same cell (merged on d and h). Arrowheads indicate the nonfused cardiomyocytes. Bars, 50 μm. (B) *LacZ*-expressing cardiomyocytes of neonatal rats were cocultured with GFP+ HUVEC (a–f) or GFP+ cFB (g–l) and stained with mouse monoclonal anti-cTnT (red) and goat polyclonal anti-GATA4 or rabbit polyclonal anti-ANF or anti-connexin43 antibodies (blue). cTnT-expressing GFP+ HUVEC (a, c, and e) and cTnT-expressing GFP+ cFB (g, i, and k) expressed GATA4 (b and h, arrowhead), ANF (d and j, arrowhead), and connexin43 (f and l, arrowhead). Bars, 50 μm.

2003; Matsuura et al., 2004). Recently, Oh et al. (2003) have reported that transplanted cardiac progenitor cells in the adult murine heart not only differentiate into cardiomyocytes, but also fuse with preexisting cardiomyocytes in the ischemia model. This finding indicates that there is another possible explanation, in which the ability to proliferate might be conferred on cardiomyocytes by surrounding proliferative noncardiomyocytes by means of cell fusion in the diseased heart. To date, two studies have been reported regarding the cell fusion between cardiomyocytes and noncardiomyocytes. Evans et al.

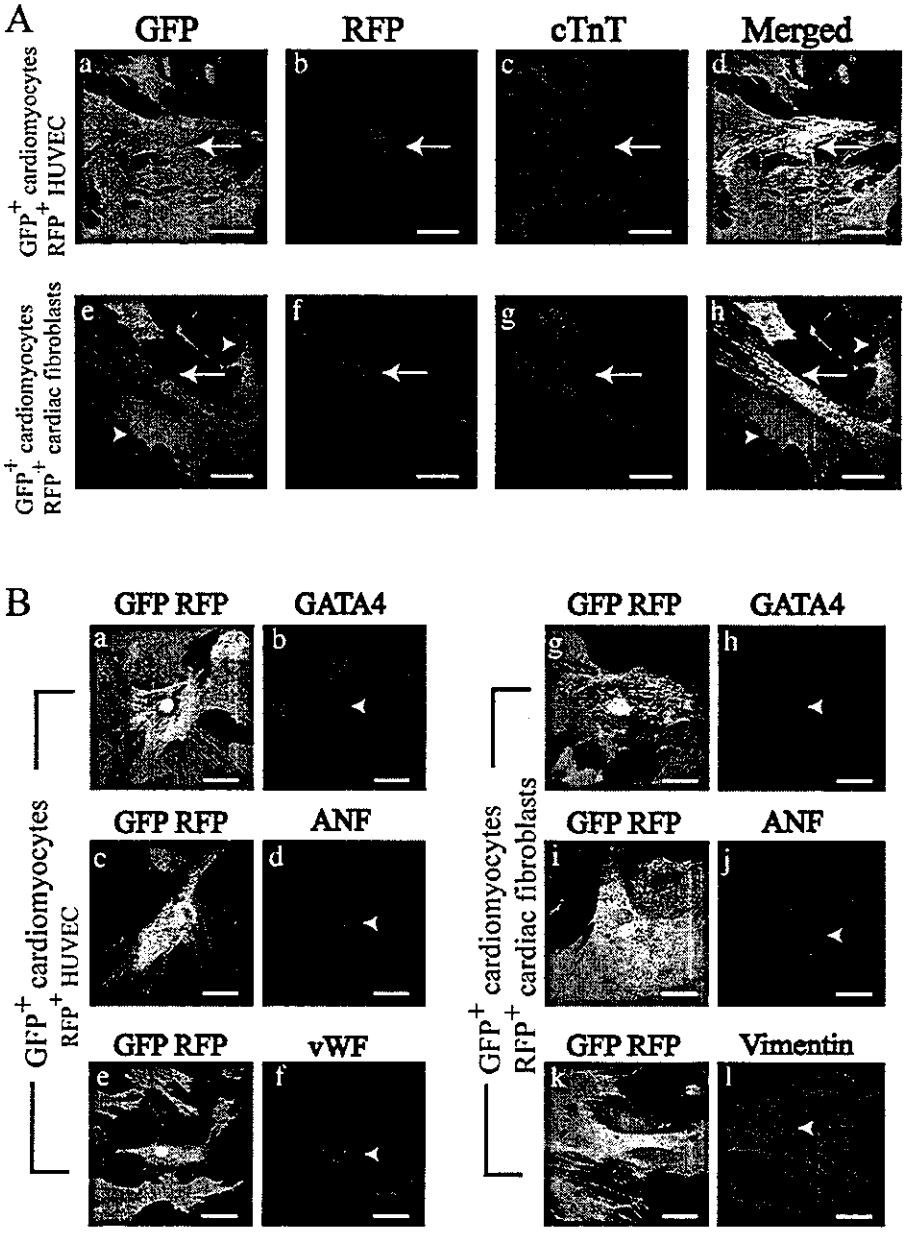

Figure 2. **HUVEC and cFB acquired the cardiac phenotype through cell fusion with cardiomyocytes.** (A) Cardiomyocytes of GFP transgenic neonatal rats were cocultured with RFP+ HUVEC (a–d) and RFP+ cFB (e–h) and were stained with mouse monoclonal anti-cTnT (blue). Merged images were obtained from the same confocal plane. RFP+ HUVEC and RFP+ cFB (b and f, arrow) expressed cardiomyocyte-derived GFP (a and e, arrow) and cTnT (c and g, arrow) in the same cell (merged on d and h). Arrowheads indicate GFP+ noncardiomyocyte. Bars, 50 μm. (B) Cardiomyocytes of GFP transgenic neonatal rats were cocultured with RFP+ HUVEC (a–f) and RFP1 cFB (g–l) and were stained with goat polyclonal anti-GATA4 or rabbit polyclonal anti-ANF, anti-vWF, or mouse monoclonal anti-vimentin antibodies (blue). GFP+/RFP+ cardiomyocyte-HUVEC fused cells (a and c) and GFP+/RFP+ cardiomyocyte-cFB fused cells (g and i) expressed GATA4 (b and h, arrowhead) and ANF (d and j, arrowhead). GFP+/RFP+ cardiomyocyte-HUVEC fused cells (e) express vWF (f, arrowhead) and GFP+/RFP+ cardiomyocyte-cFB fused cells (k) express vimentin (l, arrowhead). Bars, 50 μm.

(1994) have reported that neonatal cardiomyocytes lose their cardiac phenotypes when forced to fuse with embryonic fibroblasts by using polyethylene glycol. Alvarez-Dolado et al. (2003) have demonstrated that transplanted bone marrow cells fuse with cardiac myocytes in the heart and express cardiac contractile proteins. Currently, it is still unknown which of the mechanisms, transdifferentiation or fusion, plays a major role in phenotypic change of the cells in the heart. Therefore, it is important to examine the fusiogenic ability of cardiomyocytes with various types of cells in vivo and in vitro and to know

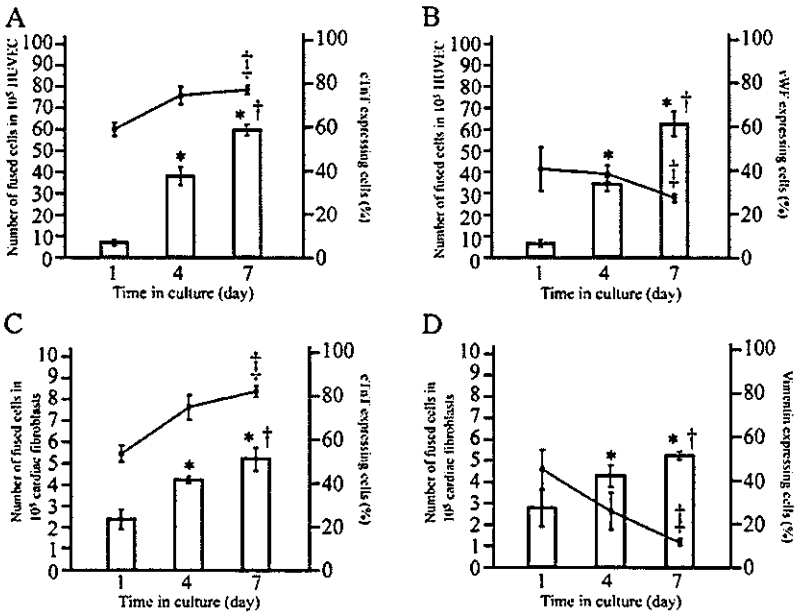

Figure 3. **Cardiac phenotype is dominated in fused cells.** (A and B) Each bar represents the number of GFP$^+$/RFP$^+$ fused cells in 10^5 RFP$^+$ HUVEC cocultured with GFP$^+$ neonatal rat cardiomyocytes at different time in culture. The number of GFP$^+$/RFP$^+$ fused cells was increased with the time-dependent manner. The percentage of cTnT-positive cells and the percentage of vWF-positive cells in GFP$^+$/RFP$^+$ fused cells are presented by line graphs. The percentage of cTnT-positive cells in GFP$^+$/RFP$^+$ fused cells (A) increased and that of vWF-positive cells (B) decreased with the time-dependent manner. Data are mean ± SD of three independent experiments. *, $P < 0.01$ vs. 1 d; †, $P < 0.01$ vs. 4 d; ‡, $P < 0.05$ vs. 1 d. (C and D) Each bar represents the number of GFP$^+$/RFP$^+$ fused cells in 10^5 RFP$^+$ cFB cocultured with GFP$^+$ neonatal rat cardiomyocytes at different time in culture. The number of GFP$^+$/RFP$^+$ fused cells was increased with the time-dependent manner. The percentage of cTnT-positive cells and the percentage of vimentin-positive cells in GFP$^+$/RFP$^+$ fused cells are presented by line graphs. The percentage of cTnT-positive cells in GFP$^+$/RFP$^+$ fused cells (C) increased and that of vimentin-positive cells (D) decreased with the time-dependent manner. Data are mean ± SD of three independent experiments. *, $P < 0.01$ vs. 1 d; †, $P < 0.01$ vs. 4 d; ‡, $P < 0.05$ vs. 1 d.

whether cardiomyocytes can obtain proliferative ability after fusion without losing cardiac phenotypes.

Here, we demonstrate that neonatal cardiomyocytes fuse with various kinds of somatic cells including human umbilical vein endothelial cells (HUVEC), cardiac fibroblasts (cFB), bone marrow cells, and endothelial progenitor cells (EPCs) spontaneously in vitro. When cardiomyocytes fused with HUVEC or cFB both phenotypes were observed at first, but cardiac phenotypes became dominant over time. Furthermore, terminally differentiated cardiomyocytes reentered the G2-M phase in the cell cycle after cell fusion with proliferative noncardiomyocytes. Cardiomyocytes spontaneously fused with transplanted HUVEC and skeletal muscle–derived cells in vivo and maintained the phenotypes of cardiomyocytes. Finally, we demonstrated that some cells in the cryoinjured heart expressed both cardiac and endothelial lineage marker proteins along with Ki67.

Results

HUVEC and cFB acquired the cardiac phenotype through cell fusion with cardiomyocytes

When GFP-expressing (GFP$^+$) HUVEC or GFP$^+$ cFB were cocultured with neonatal rat cardiomyocytes that were infected with the adenoviral vector carrying the *LacZ* reporter gene, some of GFP$^+$ HUVEC and GFP$^+$ cFB coexpressed both cardiac troponin T (cTnT) and β-galactosidase (β-gal) (Fig. 1 A, a–h, arrows). These GFP- and cTnT-expressing cells also expressed GATA4 (Fig. 1 B, a, b, g, and h, arrowheads), atrial natriuretic factor (ANF) (Fig. 1 B, c, d, i and j, arrowheads), and connexin43 (Fig. 1 B, e, f, k, and l, arrowheads). The expression of the cardiac proteins in GFP$^+$ cells was observed only in the coculture condition and all of cTnT-expressing HUVEC and cFB were positive for β-gal, suggesting that HUVEC and cFB acquired the cardiac phenotype through cell fusion with cardiomyocytes. The cTnT-positive GFP-expressing cells were found in 0.019% of GFP$^+$ HUVEC and 0.004% of GFP$^+$ cFB after 4 d of coculture. To rule out the possibility that noncardiomyocytes were infected with the adenoviral vector carrying the *LacZ* reporter gene during coculture, we examined the cell fusion by using neonatal cardiomyocytes prepared from GFP transgenic rats and red fluorescent protein-expressing (RFP$^+$) HUVEC or RFP$^+$ cFB. When RFP$^+$ HUVEC or RFP$^+$ cFB were cocultured with GFP$^+$ cardiomyocytes, some of RFP$^+$ HUVEC and RFP$^+$ cFB coexpressed cardiomyocyte-derived GFP and cTnT (Fig. 2 A, a–h, arrows). Some of both GFP- and RFP-expressing (GFP$^+$/RFP$^+$) fused cells expressed GATA4 (Fig. 2 B, a, b, g, and h, arrowheads), ANF (Fig. 2 B, c, d, i, and j, arrowheads), and connexin43 (unpublished data). Live imaging showed that GFP$^+$ cardiomyocytes fused with RFP$^+$ HUVEC beat spontaneously (see Fig. S1 and Video 1, available at http://www.jcb.org/cgi/content/full/jcb.200312111/DC1). They beat regularly and the beating rate was ~80 beats/min, which was similar to that of cocultured cardiomyocytes, suggesting that cardiomyocyte function was maintained even after fusing with other cells.

Cardiac phenotypes became predominant in fused cells

The von Willebrand factor (vWF) and vimentin are phenotype-specific markers of endothelial cells and fibroblasts, respectively, and are never expressed in cardiomyocytes. When GFP$^+$ cardiomyocytes were cocultured with RFP$^+$ HUVEC or RFP$^+$

Table I. **The phenotypic analysis of fused cells between cardiomyocytes and HUVEC**

	Number of cells in 10^5 RFP$^+$ HUVEC (% of total fused cells)		
	1 d	4 d	7 d
GFP$^+$/RFP$^+$/TnT$^+$	3.86 ± 0.64 (58.6%)	27.2 ± 4.0 (73.7%)	44.2 ± 0.7 (76.2%)[c]
GFP$^+$/RFP$^+$/TnT$^-$	2.72 ± 0.26 (41.4%)	9.7 ± 0.9 (26.3%)	13.8 ± 1.2 (23.8%)[c]
GFP$^+$/RFP$^+$	6.59 ± 0.89	36.9 ± 3.2[a]	58.0 ± 1.9[a,b]
GFP$^+$/RFP$^+$/vW$^+$	2.79 ± 0.93 (41.3%)	13.5 ± 1.8 (39.2%)	17.4 ± 1.6 (27.7%)[c]
GFP$^+$/RFP$^+$/vW$^-$	3.71 ± 0.32 (58.7%)	20.7 ± 0.6 (60.8%)	45.2 ± 4.2 (72.3%)[c]
GFP$^+$/RFP$^+$	6.49 ± 1.17	34.2 ± 3.6[a]	62.6 ± 5.9[a,b]

Times indicate period after starting coculture. Fused cells were detected as GFP$^+$/RFP$^+$ cells. Each number represents the number of cells in 10^5 RFP$^+$ HUVEC. Data are mean ± SD of three independent experiments.
[a]$P < 0.01$ vs. 1 d.
[b]$P < 0.01$ vs. 4 d.
[c]$P < 0.05$ vs. 1 d.

cFB, some of GFP$^+$/RFP$^+$ fused cells expressed vWF (Fig. 2 B, e and f) and vimentin (Fig. 2 B, k and l), respectively. To elucidate the phenotype in fused cells, we quantified the percentage of cTnT-, vWF-, or vimentin-expressing cells in the GFP$^+$/RFP$^+$ fused cells. When GFP$^+$ cardiomyocytes were cocultured with RFP$^+$ HUVEC, the number of GFP$^+$/RFP$^+$ fused cells was increased with the time-dependent manner (Fig. 3, A and B, bar graphs; Table I). The percentage of cTnT-expressing cells in the total fused cells was also increased with the time-dependent manner (d 1, 58.6 ± 2.9%; d 4, 73.7 ± 3.9%; d 7, 76.2 ± 1.9%); on the other hand, the percentage of vWF-expressing cells in fused cells was decreased with the time-dependent manner (d 1, 41.3 ± 10.3%; d 4, 39.2 ± 3.7%; d 7, 27.7 ± 1.6%), suggesting that the cardiac phenotype becomes predominant in the cells formed by fusion between cardiomyocytes and endothelial cells (Fig. 3, A and B, line graphs; Table I). When GFP$^+$ cardiomyocytes were cocultured with RFP$^+$ cFB, the number of GFP$^+$/RFP$^+$ fused cells was gradually increased (Fig. 3, C and D, bar graphs; Table II). The percentage of cTnT-expressing cells in fused cells was also increased with the time-dependent manner (d 1, 54.2 ± 3.8%; d 4, 75.8 ± 5.6%; d 7, 83.5 ± 2.6%); on the other hand, the percentage of vimentin-expressing cells (Fig. 2 B, k and l) in fused cells was decreased progressively (d 1, 45.3 ± 9.3%; d 4, 25.9 ± 8.8%; d 7, 11.5 ± 1.6%), suggesting that cardiac phenotypes also dominate in fused cells between cardiomyocytes and cFB (Fig. 3, C and D, line graphs; Table II).

Cardiomyocytes reenter the cell cycle by cell fusion with adult somatic cells in vitro

To determine whether cardiomyocytes reenter the cell cycle after fusion, we examined the expression of the cell cycle marker proteins such as Ki67, phosphohistone H3 (PH3), and cyclinB1 in fused cells. First, we examined whether monocultured HUVEC, cFB, and neonatal cardiomyocytes expressed Ki67, PH3, and cyclinB1 (Fig. 4). Many of HUVEC and cFB in the growth medium expressed Ki67, PH3, and cyclinB1 in their nuclei. Some neonatal rat cardiomyocytes expressed Ki67, but not PH3 and cyclinB1, suggesting that some neonatal cardiomyocytes are in the G1-S stage, but not in the G2-M stage of the cell cycle. However, when fused with HUVEC and cFB some cardiomyocytes expressed PH3 (Fig. 5 b for HUVEC and Fig. 5 d for cFB) and cyclinB1 (Fig. 5 f for HUVEC and Fig. 5 h for cFB). Among cardiomyocytes fused with HUVEC, ~9% of the cells expressed PH3 (Fig. 6 A). When treated for 6 h with nocodazole, an inhibitor of microtubule dynamics and cell cycle progression (Blajeski et al., 2002; Tamamori-Adachi et al., 2003), the number of PH3-expressing fused cells was increased up to ~21% in fused cells. At 3 h after the withdrawal of nocodazole, this number was decreased to ~15%. In cardiomyocytes fused with cFB (Fig. 6 B), ~14% of the cells expressed PH3, and at 24 h after the nocodazole treatment the number of PH3-expressing fused cells was increased up to ~29%. This number was decreased to ~20% at 3 h after the withdrawal of

Table II. **The phenotypic analysis of fused cells between cardiomyocytes and cardiac fibroblasts**

	Number of cells in 10^5 RFP$^+$ cardiac fibroblasts (% of total fused cells)		
	1 d	4 d	7 d
GFP$^+$/RFP$^+$/TnT$^+$	1.29 ± 0.19 (54.2%)	3.19 ± 0.20 (75.8%)	4.31 ± 0.33 (83.5%)[c]
GFP$^+$/RFP$^+$/TnT$^-$	1.08 ± 0.17 (45.8%)	1.02 ± 0.16 (24.2%)	0.86 ± 0.23 (16.5%)[c]
GFP$^+$/RFP$^+$	2.37 ± 0.31	4.21 ± 0.11[a]	5.17 ± 0.54[a,b]
GFP$^+$/RFP$^+$/Vimentin$^+$	1.28 ± 0.49 (45.3%)	1.12 ± 0.35 (25.9%)	0.59 ± 0.06 (11.5%)[c]
GFP$^+$/RFP$^+$/Vimentin$^-$	1.46 ± 0.25 (54.7%)	3.13 ± 0.20 (74.1%)	4.59 ± 0.15 (88.5%)[c]
GFP$^+$/RFP$^+$	2.74 ± 0.60	4.25 ± 0.37[a]	5.18 ± 0.14[a,b]

Times indicate period after starting coculture. Fused cells were detected as GFP$^+$/RFP$^+$ cells. Each number represents the number of cells in 10^5 RFP$^+$ cardiac fibroblasts. Data are mean ± SD of three independent experiments.
[a]$P < 0.01$ vs. 1 d.
[b]$P < 0.01$ vs. 4 d.
[c]$P < 0.05$ vs. 1 d.